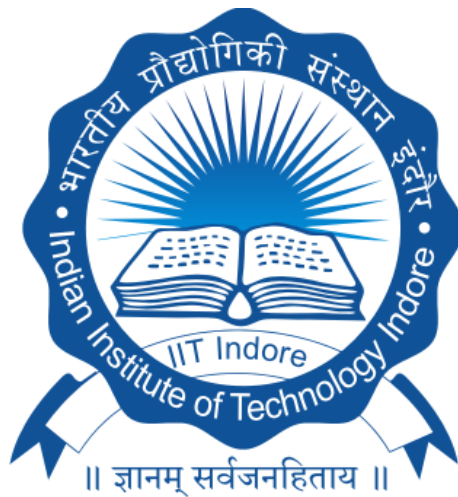


POTENTIAL OF SENTINEL - 1 AND SENTINEL - 2 FOR DEFORESTATION DETECTION

M.Tech. Thesis

By:
Shubhanshu Bishwash



DEPARTMENT OF ASTRONOMY, ASTROPHYSICS AND
SPACE ENGINEERING

INDIAN INSTITUTE OF TECHNOLOGY
INDORE

May, 2023

POTENTIAL OF SENTINEL - 1 AND SENTINEL - 2 FOR DEFORESTATION DETECTION

A THESIS

*Submitted in partial fulfillment of the
requirements for the award of the degree
of
Master of Technology*

by
Shubhanshu Bishwash



DEPARTMENT OF ASTRONOMY , ASTROPHYSICS AND
SPACE ENGINEERING

INDIAN INSTITUTE OF TECHNOLOGY
INDORE

May, 2023

INDIAN INSTITUTE OF TECHNOLOGY INDORE

CANDIDATE'S DECLARATION

I hereby certify that the work which is being presented in the thesis entitled “**Potential of Sentinel - 1 and Sentinel - 2 for Deforestation Detection**” in the partial fulfillment of the requirements for the award of the degree of MASTER OF TECHNOLOGY and submitted in the DEPARTMENT OF ASTRONOMY, ASTROPHYSICS AND SPACE ENGINEERING, Indian Institute of Technology Indore, is an authentic record of my own work carried out during the time period from June, 2022 to April, 2023 under the supervision of Dr. Unmesh Khati . The matter presented in this thesis has not been submitted by me for the award of any other degree of this or any other institute.



20/04/2023

Signature with date
(Shubhanshu Bishwash)

This is to certify that the above statement made by the candidate is correct to the best of my knowledge.



20/04/2023

(DR. UNMESH KHATI)

Shubhanshu Bishwash has successfully given his M.Tech presentation held on April 25, 2023



20/04/2023

Signature(s) of Supervisor(s) of
M.Tech thesis, Date:



Convener, DPGC

Date:- 17/05/2023

Head of Department, AASE

Date:- 17/05/2023

Dr. Priyank J. Sharma (PSPC-2)

Date:- 17/05/2023



Prof. Abhirup Datta (PSPC-1)

Date:- 17/05/2023

Dr. Saurabh Das (PSPC-3)

Date:- 17/05/2023



ABSTRACT

This M.Tech thesis explores the potential of Sentinel - 1 and Sentinel - 2 satellite data for detecting deforestation in forests. The study employs a change detection algorithm to identify and analyze changes in the forest cover. Both Sentinel - 1, which records data in the C Band SAR, and Sentinel - 2, which is an optical satellite, provide multispectral data for detecting changes in the forest cover. In this study, two bands of Sentinel - 1 and four bands of Sentinel - 2 were found to be effective in detecting forest and vegetation. The change detection algorithm was applied to these bands and combinations of them to determine which combination yielded the most effective results. The accuracy of the analysis was determined using ground truth data from two different sources. Additionally, the accuracy of the analysis for different forest types and species was evaluated separately. The results of the study demonstrate the potential of Sentinel - 1 and Sentinel - 2 satellite data for accurately detecting deforestation in forested areas. The findings of this research can be used to inform and improve forest management and conservation practices.

Contents

1	Introduction	1
1.1	Objectives	1
1.2	Significant Use Cases	2
1.3	Synopsis	2
2	Literature Review and Concept	4
2.1	Backscatter Mechanism	5
2.2	Backscatter Mechanism for VV and VH polarizations	6
2.3	Behaviour in forested areas	6
2.4	Trunk and Trunk-Ground interactions	6
2.5	Crown - Ground interaction	7
2.6	Direct Backscatter from the Ground	7
2.7	Sentinel - 2's behaviour	7
3	Area of Interest and Materials Used	9
3.1	Region of Interest	9
3.2	Sentinel - 1 Data	10
3.3	Sentinel - 2 Data	10
3.4	Ground Truth data	11
4	Methodology	12
4.1	Cummulative Sum	13
4.2	Backscatter Plots	13
4.3	Residuals and Rolling Median	15
4.4	Bootstrapping	16
4.5	Threshold and Change Map	17
4.6	Accuracy Ground truths	20
4.7	Confusion Matrix	22
5	Results and Discussion	23
5.1	Sentinel-1	23
5.1.1	VV band - Sentinel - 1	24
5.1.2	VH band - Sentinel - 1	25
5.1.3	VH / VV - Sentinel - 1	26
5.1.4	VH/[VV(VH-VV)] and (VH-VV)/(VH+VV) - Sentinel - 1	27
5.2	Sentinel-2	28
5.2.1	Band 4 - Sentinel - 2	29
5.2.2	Band 5 - Sentinel - 2	30
5.2.3	Band 6 - Sentinel - 2	31

5.2.4	Band 8 - Sentinel - 2	32
5.2.5	NDVI (Band 8 - Band 4 / Band 8 + Band 4) - Sentinel - 2	33
5.3	Accuracy Analysis Based on Type of Forest	34
5.3.1	Plantation	35
5.3.2	Dry Shivalik Sal	36
5.3.3	Moist Tarai Sal	37
5.4	Accuracy Analysis Based on the Species	38
5.4.1	Teak	39
5.4.2	Cottonwood / Poplar	40
5.4.3	Mixed-Plantation	41
6	Summary & Conclusion	42

REFERENCES

List of Figures

2.1	Optical vs. SAR side by side comparison.	5
2.2	Backscatter magnitude from a cylinder with radius less than the wavelength at different orientations with respect to incoming radar beam.	7
3.1	Optical Satellite Imagery (Top, credit: Google Earth) and SAR Imagery (Bottom) depicting the logging activity throughout the year	9
3.2	Hansen’s Global Forest cover map. The different colors depict different years	11
4.1	Behaviour of VV backscatter before and after logging of trees	12
4.2	Cumsum of the Residuals	13
4.3	Mean Backsactter Plot	14
4.4	Backscatter plot on a subset	14
4.5	Backscatter values, measured in dB (dates on the left)	15
4.6	Timeseries plot with rolling median filter	15
4.7	Residual Image	16
4.8	Bootstrap for 200 values	17
4.9	Histogram	17
4.10	S values after masking	18
4.11	Product plotted as a heatmap to visualize the regions where the change point was significant with high confidence	18
4.12	Regions with significiant change points in the data	19
4.13	Change Map, color coded according to the dates	19
4.14	Hansen Global Forest Cover Map	20
4.15	Validation Map created using QGIS	21
5.1	Change map obtained from Sentinel - 1 - VV Band	24
5.2	Change map obtained from Sentinel - 1 - VH Band	25
5.3	Change map obtained from Sentinel - 1 - VH/VV	26
5.4	Change map for $VH/[VV(VH-VV)]$	27
5.5	Change map for $(VH-VV)/(VH+VV)$	27
5.6	Change map obtained from Sentinel-2, Band 4	29
5.7	Change map obtained from Sentinel - 2, Band 5	30
5.8	Change map obtained from Sentinel - 2 - Band 6	31
5.9	Change map obtained from Sentinel - 2 - Band 8	32
5.10	Change map obtained from Sentinel - 2 - NDVI	33
5.11	Types of forests in the Area of Interest	34
5.12	Distribution of various species in the forest, the lines depict the seperation between 2 compartments	38

6.1	Change map obtained from Sentinel - 2 - Band 8 - in presence and absence of cloud cover	43
-----	---	----

List of Tables

5.1	Summary of Accuracy Analysis of Sentinel-1	23
5.2	Summary of Accuracy Analysis of Sentinel-2	28
5.3	Accuracy Analysis of Plantation type of trees in the forest - Accuracy in %	35
5.4	Accuracy Analysis of Dry Shivalik Sal type of trees in the forest	36
5.5	Accuracy Analysis of Moist Tarai Sal type of trees in the forest	37
5.6	Accuracy Analysis of Teak trees in the forest	39
5.7	Accuracy Analysis of Cottonwood / Poplar trees in the forest,	40
5.8	Accuracy Analysis of mixed plantation type of trees in the forest, accuracy in %	41
6.1	Summary of Type and Species-wise accuracy	42

Chapter 1

Introduction

Deforestation is a major environmental concern, and detecting changes in forest cover is critical for effective management and conservation. The use of satellite data has provided a valuable tool for monitoring changes in forest cover over large areas. In particular, the Sentinel - 1 and Sentinel - 2 satellites have the potential to provide valuable insights into forest cover changes. Sentinel - 1, which is a C-band synthetic aperture radar (SAR) satellite, is particularly useful in detecting changes in the presence and absence of trees, as its backscatter is influenced by the ground conditions, including the structure of the forest canopy.

Furthermore, Sentinel - 1 is not affected by weather conditions, making it an ideal tool for detecting changes in forest cover throughout the year. Sentinel - 2, which is an optical satellite, can provide additional bands of data to improve the accuracy of change detection algorithms, particularly in areas where the canopy structure is less dense. In this project, we explore the potential of Sentinel - 1 and Sentinel - 2 satellite data for detecting deforestation, using a change detection algorithm applied to the backscatter data obtained from these satellites.

1.1 Objectives

- Analyze and process Sentinel - 1 and Sentinel - 2 satellite data for the study area.
- Evaluate the effectiveness of different combinations of Sentinel - 1 and Sentinel - 2 bands for detecting deforestation using a change detection algorithm.
- Compare the accuracy of the change detection algorithm with ground-truth data obtained from different sources.
- Perform accuracy analysis for species and forest type separately using the obtained results.
- Identify areas of deforestation and characterize the spatial and temporal patterns of forest cover changes in the study area.[8]

1.2 Significant Use Cases

- Monitor changes in forest cover over time: With the ability to analyze and process Sentinel - 1 and Sentinel - 2 satellite data, your project can be used to monitor changes in forest cover over time. By identifying areas of deforestation and characterizing the spatial and temporal patterns of forest cover changes, your project can help track changes in forest cover and inform forest management strategies.[19]
- Aids in estimating carbon stocks in forested areas: Deforestation is a major contributor to greenhouse gas emissions and climate change. By identifying areas of deforestation and tracking changes in forest cover, your project can be used to estimate carbon stocks in forested areas. This information can be used to inform climate change mitigation strategies and support efforts to reduce greenhouse gas emissions.[4]
- Identifies areas of high conservation value and informs conservation strategies: Forests provide essential ecosystem services, including biodiversity conservation and watershed protection. By identifying areas of high conservation value, your project can inform conservation strategies and support efforts to protect and restore forest ecosystems.[2]
- Helps monitor and combat illegal logging: Illegal logging is a major driver of deforestation, biodiversity loss, and carbon emissions. By identifying areas of deforestation and monitoring changes in forest cover, your project can support efforts to combat illegal logging and promote sustainable forest management. Your project can also help identify areas at high risk of illegal logging, enabling targeted interventions and enforcement efforts. [13]

1.3 Synopsis

- Chapter 2: This chapter focuses on the fundamentals of electromagnetic (EM) waves and their interaction with physical structures. It provides a detailed discussion on the polarizations of synthetic aperture radar (SAR), and how EM waves interact with trees.
- Chapter 3: This chapter describes the area of interest and the materials used in the study. It also provides information on the data sources and ground truth data used for the research.
- Chapter 4: This chapter focuses on the preprocessing, calibration, and other steps involved in analyzing the data. It describes the behavior of backscatter with changes in ground conditions and provides insight into the cumsum method used in the study. This chapter also includes backscatter plots and discussions on the products generated.

- Chapter 5: This chapter presents the change maps obtained for all the bands and the combination of bands. It also provides an accuracy analysis of the results with ground truth data. This chapter offers insight into the effectiveness of different combinations of bands in detecting deforestation using a change detection algorithm.
- Chapter 6: This chapter provides the conclusions derived from the present study. It summarizes the main findings of the thesis, including the effectiveness of SAR in monitoring changes in forest cover, the importance of ground truth data, and the utility of different combinations of bands in detecting deforestation.

Chapter 2

Literature Review and Concept

Aquino, C., et al. "Reliably Mapping the Location, Time and Magnitude of Low-intensity Forest Disturbance using a Simple Satellite Radar Method."

frontiers - This paper proposes a straightforward and efficient approach for taking advantage of Sentinel-1 VV-polarized time data to identify small-scale disturbances in multistoried, thick tropical woods. The location, timing, and magnitude of the disturbances were determined using the Cumulative Sum (CuSum) algorithm, and the findings were confirmed by extremely precise in-situ measurements of forest canopy loss obtained using a combination of UAV LiDAR, TLS, and field inventory surveys in two different tropical forests located in Gabon and Peru. The project captured finer and more widespread tropical forest disturbances than existing forest monitoring technologies like the SAR-based RADD system and the Landsat-based GFW tool. The method can potentially be applied to measure other kinds of forest dynamics, such regrowth in forests, and it could be generalised to the regional scale. Overall, this study offers insightful information for managing and monitoring forests, particularly in light of the growing demand for agricultural and forestry products throughout the world and the ensuing deforestation and fragmentation.

The Sentinel-1 mission and its application capabilities - Torres et.al - Researchgate

- An overview of the Sentinel-1 mission, which was created by the European Space Agency (ESA) in response to operational SAR data needs identified by the EU-ESA Global Monitoring for Environment and Security (GMES) programme, is provided in the article. Sentinel-1 is a constellation of imaging synthetic aperture radar satellites operating in the C-band. The mission maintains essential instrument qualities including stability and accurate, well-calibrated data outputs and draws on ESA's legacy and expertise with the ERS and ENVISAT SAR sensors. It also provides continuity of C-Band SAR data to applications. The paper emphasises the use of SAR data as an additional or backup data source during bad weather when optical imaging is not available.

Performance Evaluation of UAVSAR and Simulated NISAR Data for Crop and Noncrop Classification Over Stoneville, MS. S. Kraatz et.al

- With the help of data gathered by NASA's airborne Uninhabited Aerial Vehicle SAR (UAVSAR) platform and simulated NISAR data, this research assesses the NASA ISRO SAR (NISAR) Cropland Area product. The study investigates crop/noncrop classifications at various spatial resolutions and coefficient of variation (CV) thresholds using mode 129A for global-scale mapping. The analysis concludes that employing UAVSAR at 10 m resolu-

tion results in the maximum accuracy of 85 %, while NISAR data at 30 m and 100 m resolutions might match the mission accuracy requirement of 80 %. The work also demonstrates that accurate agricultural products may be created at smaller spatial resolutions and that overall accuracy may not be the most sensitive parameter for classification performance.

2.1 Backscatter Mechanism

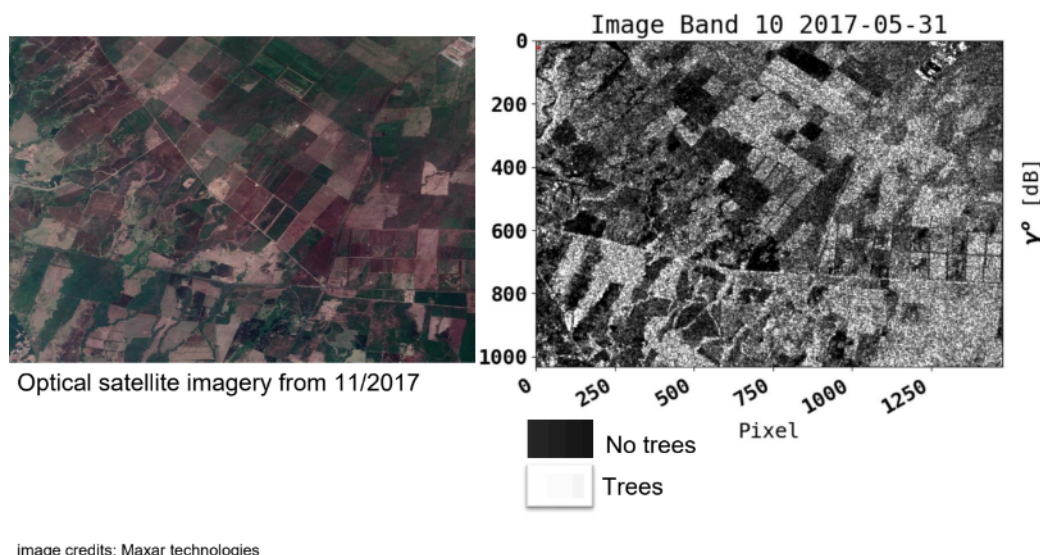


Figure 2.1: Optical vs. SAR side by side comparison.

When a radar beam hits a surface, it is both reflected and transmitted from the surface. The magnitude of the reflection depends on the degree of discontinuity in the dielectric constant at the surface. Additionally, the roughness and orientation of the surface affect the direction of reflection and the amount of energy scattered back to the source. For example, in the case of water, the change in dielectric constant causes a strong reflection. However, since the surface of water is relatively smooth, the reflection is directed away from the source, resulting in low backscatter readings. The interaction between a surface and microwave radiation depends on the wavelength of the microwave and the angle at which the radar beam strikes the surface. When the surface is smooth relative to the wavelength, most of the incident energy is scattered forward in a classical reflection direction, while a small fraction is scattered back towards the radar, with the amount of backscattering strongly dependent on the incident angle, especially at small angles. However, as the surface becomes rougher relative to the wavelength, more energy is reflected in different directions, including backwards towards the sensor. With increasing surface roughness, the angular dependence of the backscattering decreases, meaning that the amount of energy reflected back to the radar becomes less sensitive to the incident angle.

2.2 Backscatter Mechanism for VV and VH polarizations

The polarization of a radar signal affects how it interacts with the elements of a target. Vertically polarized signals are more likely to be scattered by vertical elements, while horizontally polarized signals are more likely to be scattered by horizontal elements. The complexity of the target also affects the polarization of the scattered signal. For example, a complex tree canopy will cause both vertically and horizontally polarized signals to appear similar.

The angle of incidence of the radar signal also affects the backscatter from a target. Depolarization occurs when the scattered wave has a different polarization than the incident wave. This can occur when there is multiple scattering within a target structure. For a locally flat surface, backscatter only occurs at normal incidence. However, scatter from surfaces that are the same size or smaller than the wavelength can also cause depolarization. Canopy volume scattering is a significant source of depolarized scatter.

2.3 Behaviour in forested areas

The backscatter from forested terrain can be contributed by several mechanisms. These include crown-scattering, which involves multiple scattering within the crown and is referred to as crown volume scattering. Additionally, direct backscattering can occur from the trunk and ground. Crown-ground and trunk-ground double bounces can occur in both directions, and backscatter may occur from the ground to the tree and back to the ground. However, backscatter from beneath the canopy is often attenuated as it travels back towards the radar system. Factors such as surface roughness, soil moisture, slope, and the presence of understory vegetation can influence the interaction of radar signals with the ground. The magnitude of each backscatter component depends on radar wavelength, polarization, angle of incidence, and various terrain and canopy parameters.

2.4 Trunk and Trunk-Ground interactions

In synthetic aperture radar (SAR) imaging of forested areas, direct scatter from the trunks is usually minimal due to the large incident angles of the radar relative to the vertical trunks and the smoothness of the trunk surface, particularly at the bark-wood boundary. However, in some cases, the trunk-ground double bounce can be an important or even dominant scattering interaction. Backscatter modeling studies have shown that trunk-ground double bounce can significantly contribute to the total backscatter and is sensitive to ground backscatter. Forest backscatter models provide insights into the nature and magnitude of trunk-ground interactions. A tree trunk rising perpendicular from a flat ground surface is often considered a dihedral corner reflector, resulting in attenuated backscatter. [5]

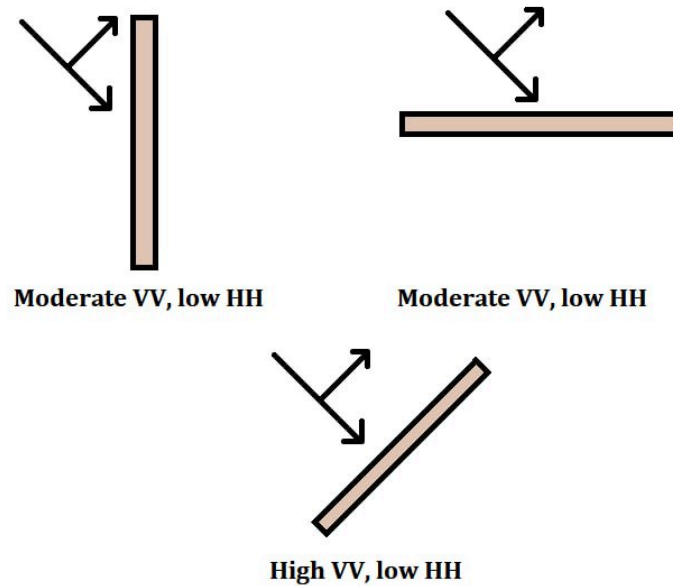


Figure 2.2: Backscatter magnitude from a cylinder with radius less than the wavelength at different orientations with respect to incoming radar beam.

2.5 Crown - Ground interaction

This interaction occurs through volume scattering and surface scattering from the branches. The magnitude of backscatter in this case is influenced by terrain factors such as surface roughness and soil moisture, but is generally smaller compared to crown volume backscatter and trunk-ground interaction. Unlike trunk-ground interaction which exhibits a corner reflector effect, the crown-ground backscatter includes a significant cross-polarized component.[5]

2.6 Direct Backscatter from the Ground

The amount of direct backscatter from the ground is influenced by various factors, such as the roughness of the surface, the moisture content, the type of ground material, the local slope, and the presence of vegetation, deadfall, and other surface perturbations. Rougher surfaces and materials with higher dielectric constants tend to produce greater backscatter. The level of backscatter is also affected by the penetration of radar waves through the forest canopy, which depends on factors such as the thickness and openness of the canopy. Additionally, the angle at which the radar is incident plays a crucial role in the amount of direct ground scattering, with higher incident angles resulting in decreased backscatter. Generally, direct ground backscatter is not a significant contributor to overall backscatter at incident angles greater than 20 degrees, except in open forest stands.[5]

2.7 Sentinel - 2's behaviour

Sentinel-2 is a multispectral satellite system that can provide valuable information on the characteristics of forests and vegetation. The bands 4 (red), 5 (near-infrared),

and 6 (shortwave infrared) are particularly useful for monitoring vegetation health and dynamics.[17] Band 4 is sensitive to chlorophyll content and can be used to estimate vegetation density and vigor. Band 5 is useful for vegetation indices such as the Normalized Difference Vegetation Index (NDVI) and can detect subtle changes in vegetation growth and health. Band 6 is sensitive to moisture content in vegetation, making it useful for detecting water stress and forest fires. The better resolution of Sentinel - 2 comes handy in performing change detection.

Chapter 3

Area of Interest and Materials Used

The project utilizes data from both Sentinel-1 and Sentinel-2 satellites to analyze the Haldwani forest in Uttarakhand, India.[23] The forest is renowned for its managed logging for industrial purposes, rendering it an ideal area for the analysis. The data utilized in the study covers the period of 2017, and was captured by Sentinel-1 and Sentinel-2 satellites. The data obtained from Sentinel-1 and Sentinel-2 for this project is particularly valuable, as it is freely available and has a high temporal and spatial resolution.

3.1 Region of Interest

Here is a satellite image of the region of interest:

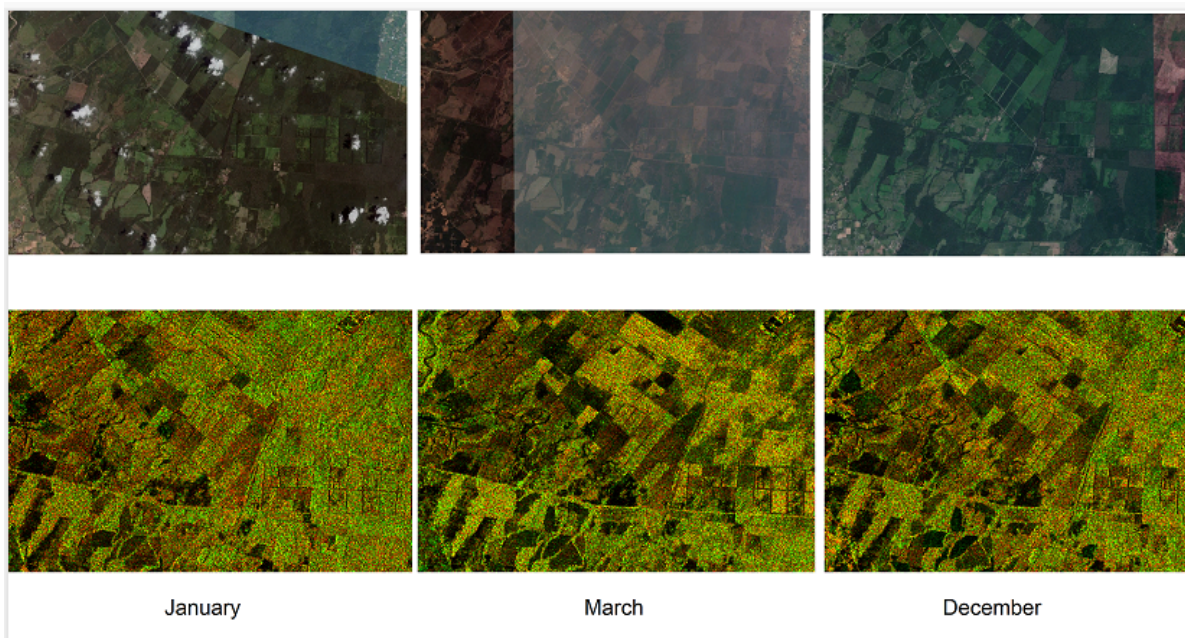


Figure 3.1: Optical Satellite Imagery (Top, credit: Google Earth) and SAR Imagery (Bottom) depicting the logging activity throughout the year

The satellite image of the area of interest reveals that the region is divided into compartments where planned tree plantations take place. The trees in these compartments are periodically logged, making this region an ideal site for change detection analysis.[25] [16]

The distinct compartments in the region facilitate the monitoring of changes in tree cover and forest structure over time, providing valuable insights into forest management practices. The periodic logging of trees in the compartments creates a unique opportunity to analyze the effects of logging on forest health and recovery.[1]

Moreover, the presence of logged areas in the region also allows for the assessment of deforestation rates and the extent of forest degradation in the region. The use of satellite data in this analysis enables the detection of changes in forest cover and structure that may not be easily observable from ground-level surveys.

3.2 Sentinel - 1 Data

Sentinel - 1- It has two polarizations, Vertical Vertical (VV) and Vertical Horizontal (VH), and offers different image modes with varying spatial resolution and swath.[26] [6]

The spatial resolution for Sentinel-1 data ranges from 5 meters to 40 meters, depending on the mode and polarization. The following are the central frequencies and spatial resolutions for Sentinel-1 VV and VH bands, both the band are C band with 10m resolution. [15]

3.3 Sentinel - 2 Data

Sentinel - 2- Sentinel-2 has a spatial resolution of 10 meters for its four visible and near-infrared bands, which include bands 4, 5, 6, and 8.[15]

These four bands have the following central wavelengths and corresponding spatial resolutions:

Band 4 (Red): 665 nm, 10 meters

Band 5 (Vegetation Red Edge): 705 nm, 10 meters

Band 6 (Vegetation Red Edge): 740 nm, 10 meters

Band 8 (Near Infrared): 842 nm, 10 meters

3.4 Ground Truth data

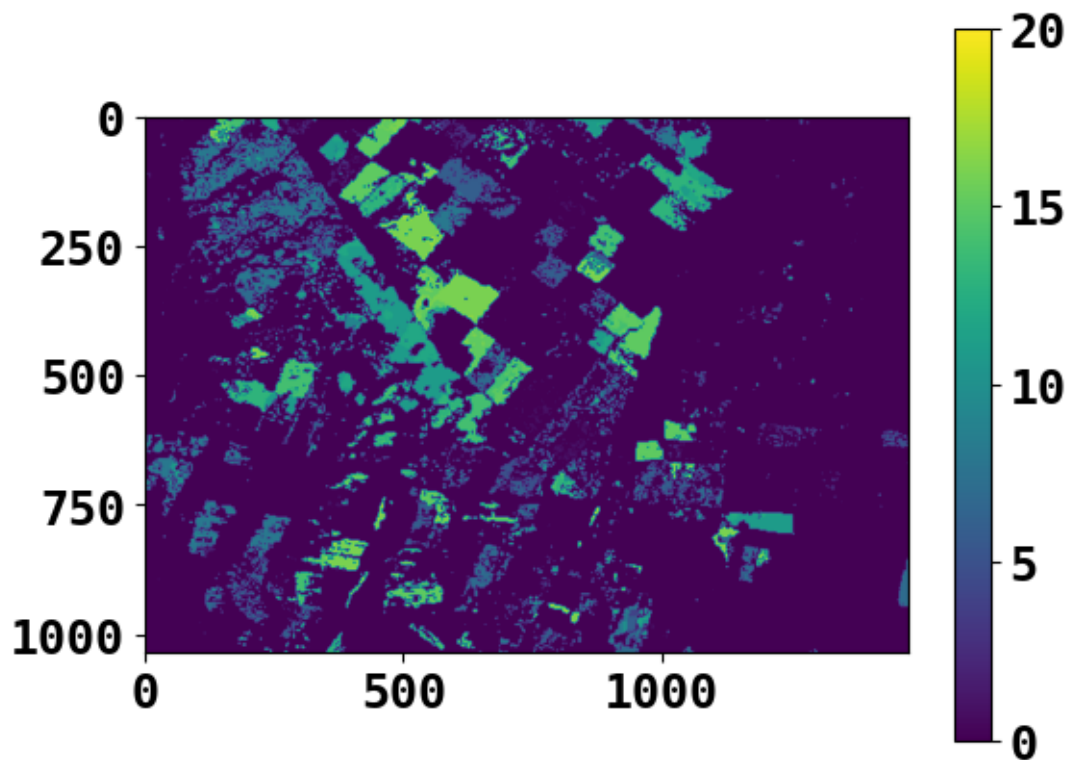


Figure 3.2: Hansen's Global Forest cover map. The different colors depict different years

The map has a spatial resolution of 30 meters, which means that each pixel in the map represents an area on the ground of 30 meters by 30 meters. The map covers the entire globe, including both terrestrial and coastal forests.

The dataset provides information on the extent and density of forest cover, as well as changes in forest cover over time. This global forest cover map was created using optical imagery.

In addition to using Hansen's Global Forest Map, a shapefile was created in QGIS to identify areas that have undergone changes and areas that have not. This was achieved by analyzing both SAR and Optical imagery of the forest. The shapefile provides a visual representation of the forest cover changes and allows for a more precise identification of areas where forest cover has been affected.

Chapter 4

Methodology

In SAR remote sensing, the Interferometric Wide swath (IW) mode captures a wide area of around 250 km at once. However, we are often interested in a smaller area within this swath. Therefore, we take a subset of the area of interest. Before analyzing the backscatter values of the SAR image, it is necessary to perform radiometric calibration using tools like SNAP. This calibration process helps to convert the pixel values of the SAR image into radar backscatter values of the scene. This conversion makes it easier to interpret the data for scientific analysis. In addition, range Doppler terrain correction is applied to account for foreshortening and overlay effects that can occur in SAR imagery due to topography. By performing these necessary steps, we can ensure accurate and meaningful interpretation of the SAR data for various applications such as land cover classification, change detection, and environmental monitoring. Here is a cropped version of the region where the deforestation (and subsequent reduction of back-scatter) has occurred. A Virtual Raster File (VRT) was created using the Geospatial Data Abstraction

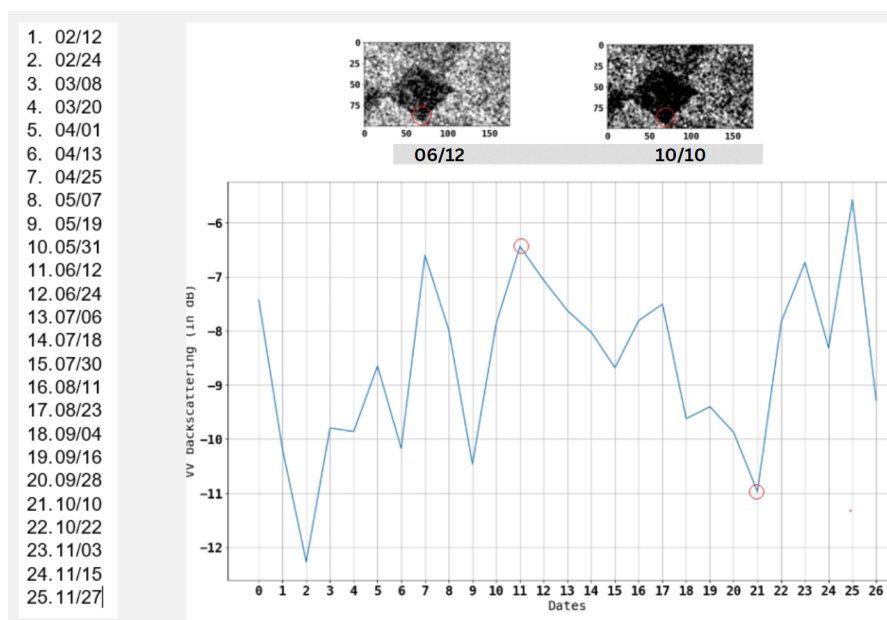


Figure 4.1: Behaviour of VV backscatter before and after logging of trees

Library (GDAL) for both Sentinel-1 and Sentinel-2 satellite images. Each layer of the VRT file corresponded to a specific date of the satellite image capture. This allowed for easier handling and organization of the large amounts of image data.

4.1 Cumulative Sum

After calculating the residuals R by subtracting the smoothed time series from the original time series, we calculate the cumulative sum of the residuals, S , which gives us an indication of how much the time series has deviated from its long-term average over time.[11] This helps to identify periods of anomalous behavior or significant changes in the backscatter magnitude over the time period of interest [12].

In our case, $S = \sum_{i=1}^n R_i$

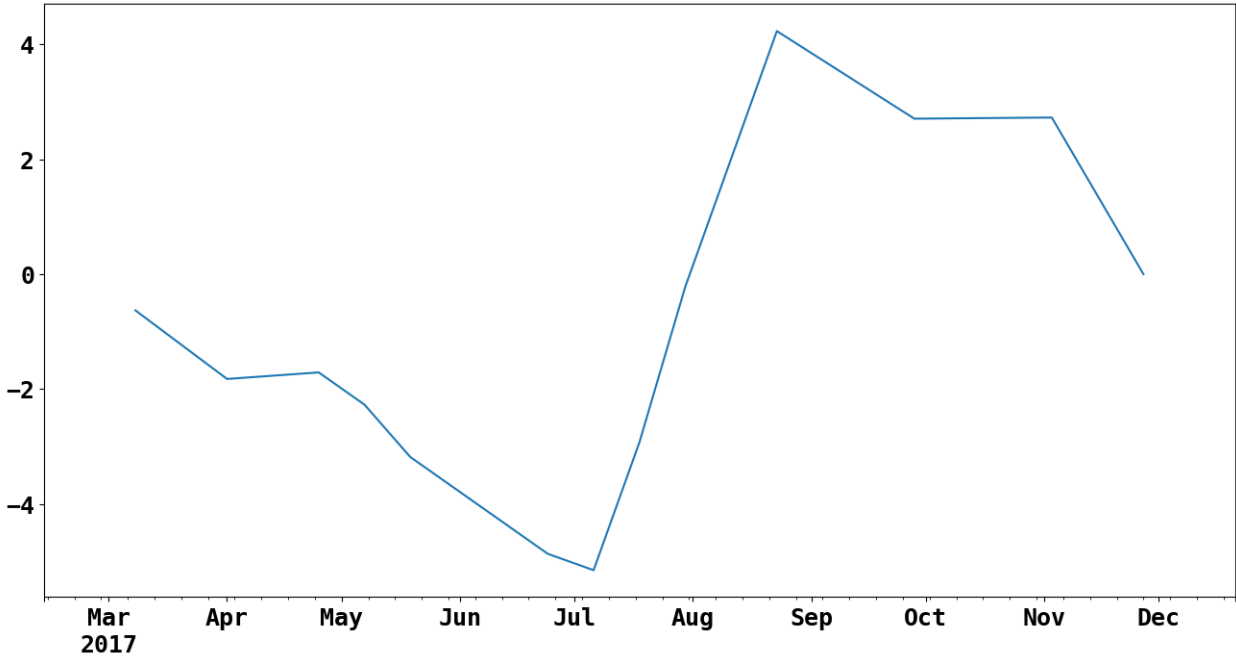


Figure 4.2: Cumsum of the Residuals

4.2 Backscatter Plots

We compute the mean backscatter coefficient for each image, converts it to decibels (dB), and then creates a time series plot of the mean backscatter coefficient over time.[7] [24]

The time series plot shows the variation of the mean backscatter coefficient over time, with each data point representing the mean value for a particular SAR image. The x-axis represents time, and the y-axis represents the mean backscatter coefficient in decibels (dB).[18]

Additionally, each data point is labeled with the corresponding band number, which represents the order in which the SAR images were acquired.[10]

Overall, this time series plot can be useful for monitoring changes in the backscatter coefficient of the target area over time, which can in turn be used to infer changes in land cover, moisture content, and other environmental factors. [3]

We can observe the backscatter over a smaller region and visualize it like this: We first extract the subset of the SAR data based on the subset definition, and then calculates the mean backscatter coefficient for each time step along the time series axis

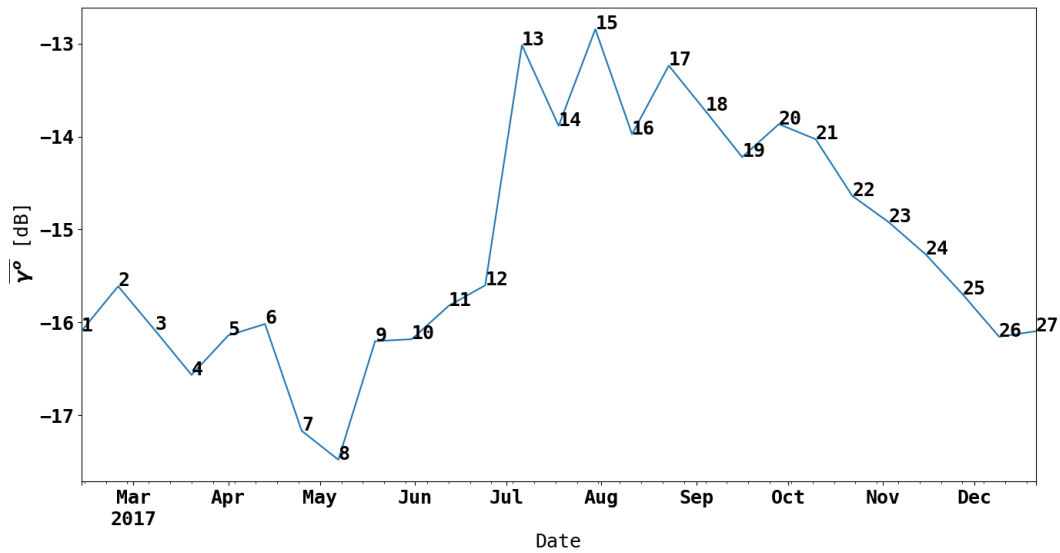


Figure 4.3: Mean Backscatter Plot

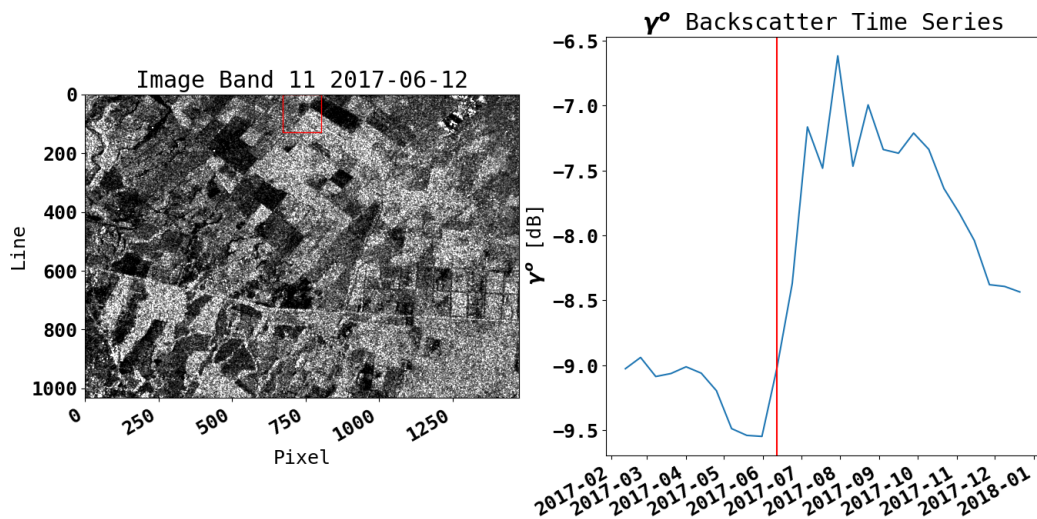


Figure 4.4: Backscatter plot on a subset

(axis=0), resulting in a 1D numpy array of mean backscatter values. The mean backscatter values are then converted to dB and stored in a pandas time series object (ts) with the datetime index.

The time series object (ts) can be plotted using the plot method of the time series object, which generates a line plot of the mean backscatter values over time.

The time series of mean backscatter values can provide information on changes in the backscatter coefficient over time, which can be related to changes in land cover and other surface properties.

17/05/2023

2017-02-12	-19.317835
2017-02-24	-16.567427
2017-03-08	-16.561108
2017-03-20	-18.294216
2017-04-01	-12.359146
2017-04-13	-15.337107
2017-04-25	-21.830841
2017-05-07	-13.215885
2017-05-19	-18.011383
2017-05-31	-16.628815
2017-06-12	-16.756094
2017-06-24	-16.053692
2017-07-06	-9.242913
2017-07-18	-21.986162
2017-07-30	-10.005383
2017-08-11	-10.891999
2017-08-23	-9.042276
2017-09-04	-16.515779
2017-09-16	-17.740177
2017-09-28	-16.262093
2017-10-10	-15.487329
2017-10-22	-12.668177
2017-11-03	-12.004250
2017-11-15	-18.497940
2017-11-27	-21.884541
2017-12-09	-18.150206
2017-12-21	-15.813356

Figure 4.5: Backscatter values, measured in dB (dates on the left)

4.3 Residuals and Rolling Median

The time series data is first filtered using a rolling median filter with a window size of 5, and both the filtered and unfiltered data are plotted. The residual gives us the value of R that we used in the Cusum formula. This can be useful for visualizing the variation of backscatter magnitude over time for a specific subset of data, and for identifying any trends or patterns in the data. The comparison of the time series data with its mean can also provide insights into any deviations or anomalies in the data.

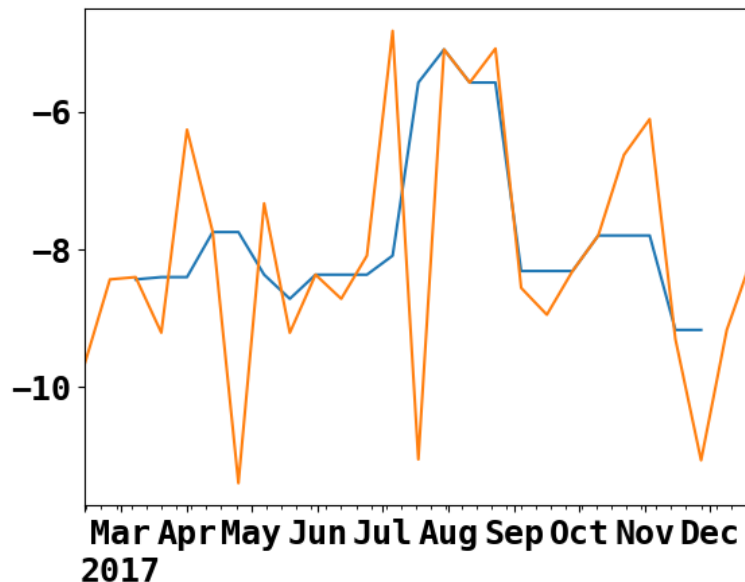


Figure 4.6: Timeseries plot with rolling median filter

About rolling median filter: The rolling median function is a type of filter that is used to smooth out time series data by reducing high frequency noise and random fluctuations. The function calculates the median of a window of data points (in this case, a window

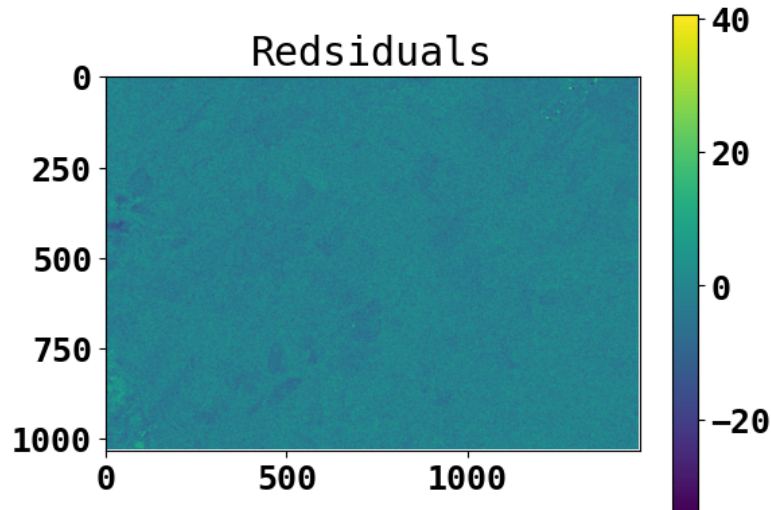


Figure 4.7: Residual Image

of size 5), and moves the window along the time series to create a filtered version of the data.

The rolling median function is often used instead of other types of filters (such as the rolling mean or moving average filters) when dealing with time series data that contains extreme values or outliers, as the median is more robust to such values. It can also be more effective at preserving sharp transitions or edges in the data.

In this specific project, the rolling median function is used to smooth out the time series data and make any trends or patterns more apparent, while reducing the effect of noise or random fluctuations in the data. The filtered and unfiltered data are both plotted for comparison purposes, to help visualize the impact of the filter on the time series.

4.4 Bootstrapping

The bootstrap method was used to estimate the distribution of the maximum difference in the cumulative sum of residuals (Sdiff) that could be obtained by chance, assuming that there was no real change point in the data. This was done by randomly permuting the time series data (i.e., randomly shuffling the residuals), and then calculating the Sdiff for each permuted series. By repeating this process multiple times (here, n number of bootstraps=200), we obtained a distribution of Sdiff values that could be expected by chance. We could then compare the observed Sdiff value (calculated earlier for the original, unpermuted data) to this distribution to estimate the probability of obtaining such a large Sdiff value by chance alone. If this probability was small (e.g., less than 0.05), we could conclude that there was likely a real change point in the data.

Confidence Level for change point 99.5 percent

Change point significance metric: 0.8246569366095272

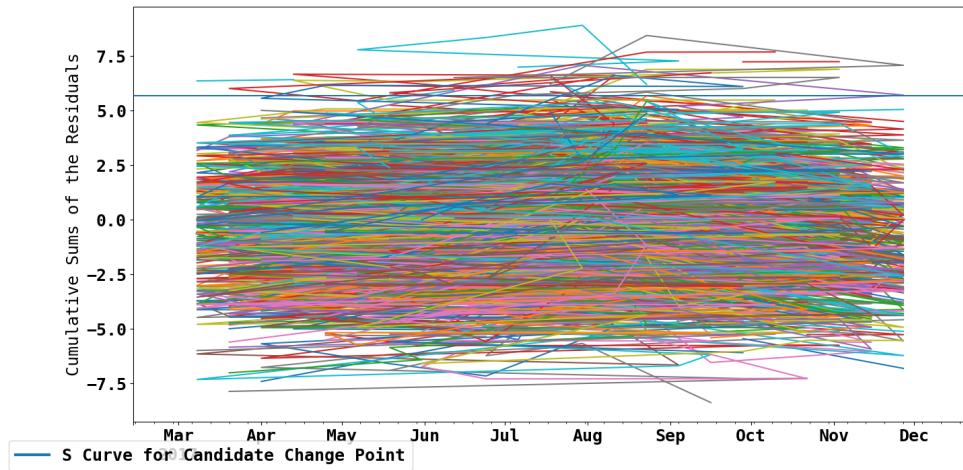


Figure 4.8: Bootstrap for 200 values

4.5 Threshold and Change Map

We calculate the cumulative sum of the residuals (R), and then calculate the maximum and minimum cumulative sum along the time axis.[22] The difference between these two values (S_{max} and S_{min}) gives the maximum change in cumulative sum between any two time points, which is then stored in S_{diff} . [21]

The code then creates a figure with three subplots, each showing a different image: S_{max} , S_{min} , and S_{diff} . The v_{min} and v_{max} arguments set the minimum and maximum values for the color scale of the images, respectively.[14]

Finally, a histogram of the values in S_{diff} is generated using the `hist` function from `matplotlib.pyplot`. The x-axis represents the range of values for the S_{diff} variable and the y-axis represents the frequency of occurrence for each bin in the histogram. [20]

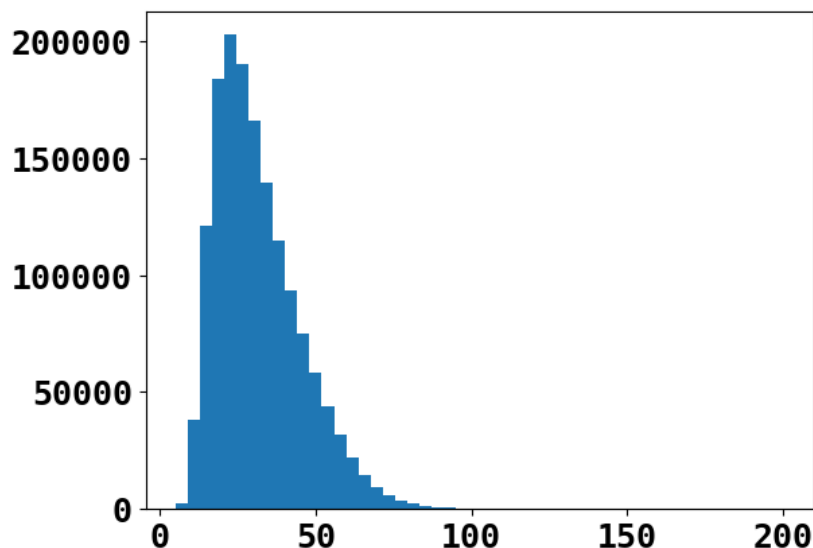


Figure 4.9: Histogram

We can set the threshold value for the change point detection algorithm to a certain percentile of the histogram of the S_{diff} values.

Alternatively, we can manually assign the value of threshold at maximum accuracy, if we have the ground truth data. [9]

Here is what the Sdiff looks after the masking:

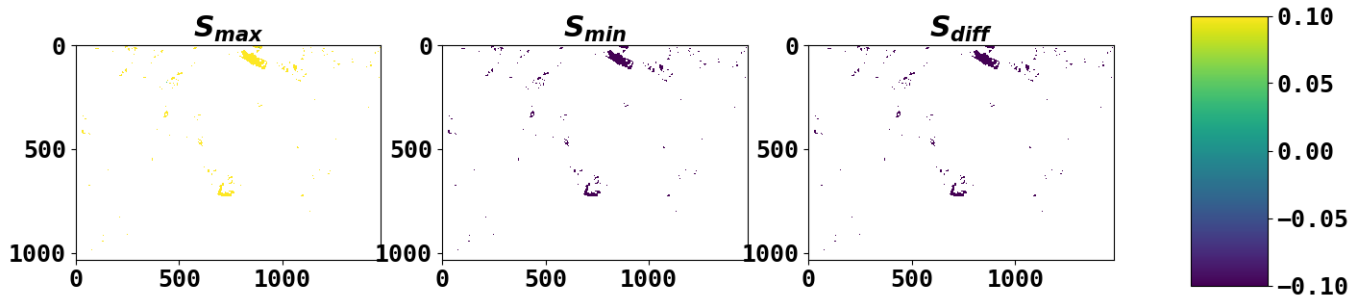


Figure 4.10: S values after masking

The second bootstrap was done to estimate the confidence level and significance of the change point detection. In this case, a masked array was used to exclude time periods that were not significant. The randomization was done by shuffling the time index of the masked array. The maximum and minimum cumulative sums of the residuals were calculated for each bootstrapped sample, and the maximum difference between the two was computed as the Sdiff value.

The maximum Sdiff value was then compared with the previous maximum value, and if it was greater, it was assigned as the new maximum value. Additionally, a count was kept of how many times the bootstrapped Sdiff value was less than the original Sdiff value. This count was used to estimate the confidence level of the change point detection.

Finally, the product of the confidence level and the significance of the change point detection was obtained by multiplying the confidence level and the significance values computed in the previous step. This product was plotted as a heatmap to visualize the regions where the change point was significant with high confidence.

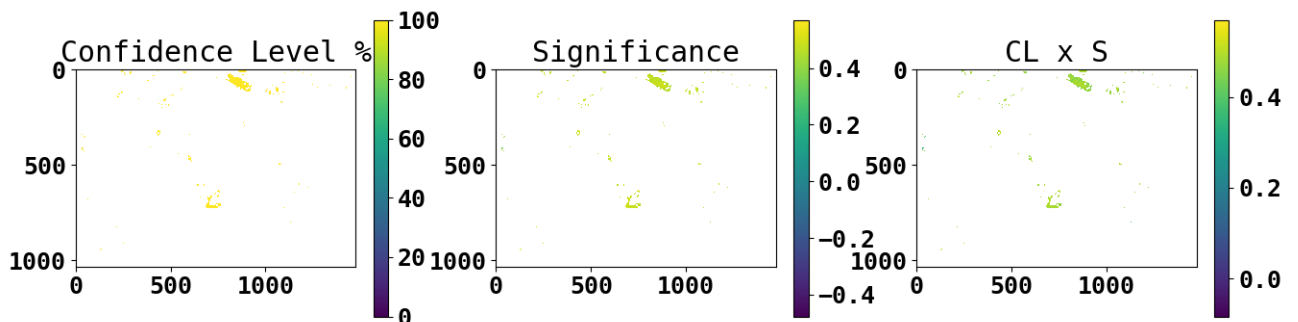


Figure 4.11: Product plotted as a heatmap to visualize the regions where the change point was significant with high confidence

The code generates a binary image where pixels with a value less than cp-thres are set to True (white). The input to plt.imshow is the boolean array $CL * CP - significance \geq cp - thres$, which is the element-wise multiplication of the confidence level (CL) and significance arrays, compared with the threshold value cp-thres. The resulting image can be used to identify regions with significant change points in the data.

The index of the maximum value along the time axis is then computed for each pixel in

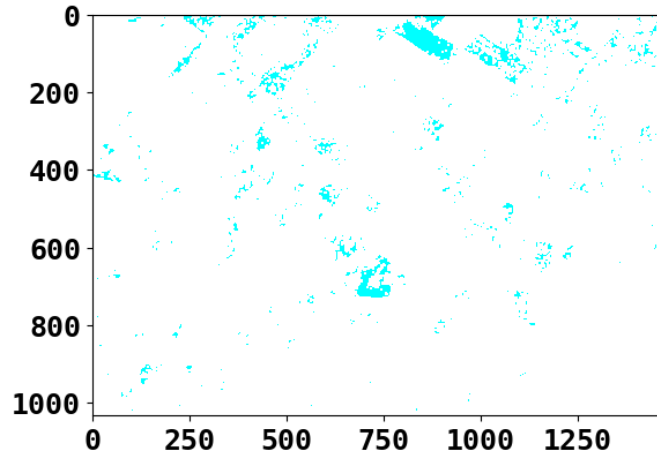


Figure 4.12: Regions with significant change points in the data

the array. The resulting indices are then used to find the dates of change by looking up the dates from the time index array (`tindex`). The resulting change indices and dates are stored in the variables `change-indices` and `change-dates`, respectively.

Finally, a color map is chosen, and a figure with an image plot of the change index array (CP-index) and a color bar are created using `plt.subplots` and `plt.imshow`. The tick labels for the color bar are set to the change dates, and the orientation of the color bar is set to horizontal. The resulting image plot shows the dates of significant change points in the time series data.

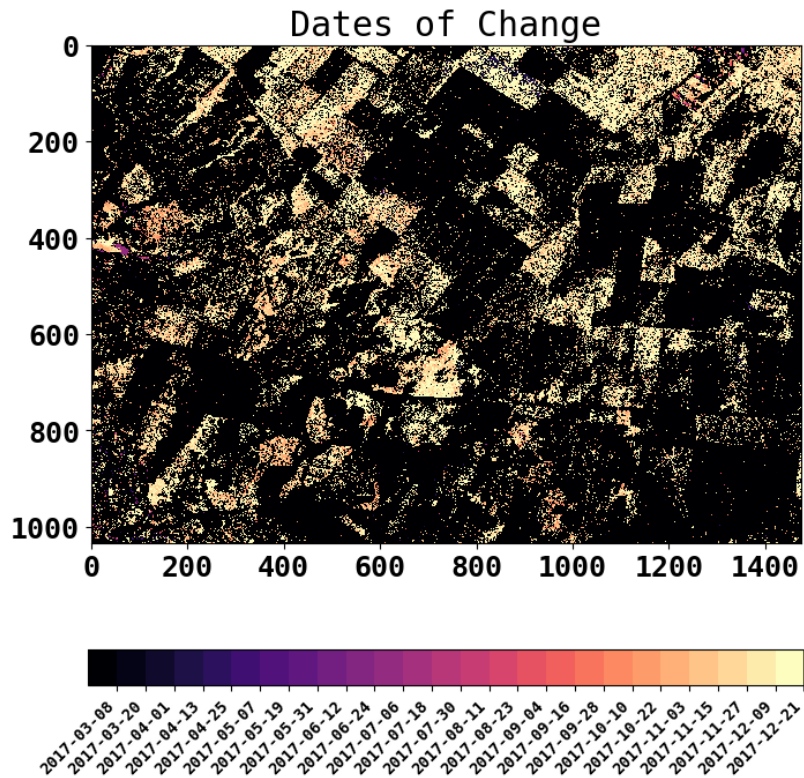


Figure 4.13: Change Map, color coded according to the dates

4.6 Accuracy Ground truths

1. Hansen Global Forest cover:

Hansen Global Forest cover was used for accuracy analysis as ground truth. This data was in several layers, each representing a different year. Hansen Forest Change map (hfc) that are less than 17 or greater than or equal to 18 are set to zero. This means that all the layers of the map, except layer 17, are masked out. Then, the values that are equal to 17 are set to 1, effectively creating a binary mask of layer 17. Finally, `plt.imshow` is used to display this binary mask, with a gray colormap, showing the areas with deforestation in 2017 as white and the non-deforested areas as black. This is a common technique to visualize specific layers or bands of multi-band images, and this is how the data of 2017 was extracted.

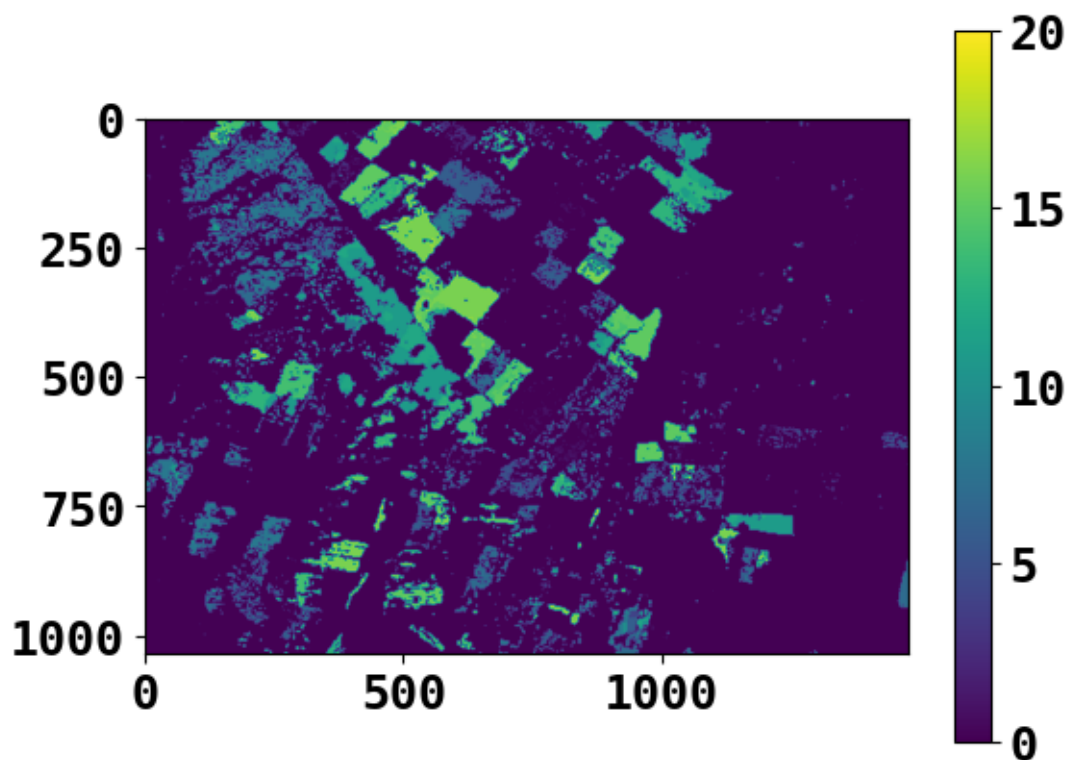


Figure 4.14: Hansen Global Forest Cover Map

2. QGIS validation map:

To obtain another reference point for ground truth, a shapefile was generated using QGIS to distinguish between areas that have undergone changes and areas that have not. This was achieved by examining both SAR and Optical imagery of the forest, which enabled a more accurate identification of regions where forest cover has been impacted. The resulting shapefile provides a visual representation of the forest cover changes.

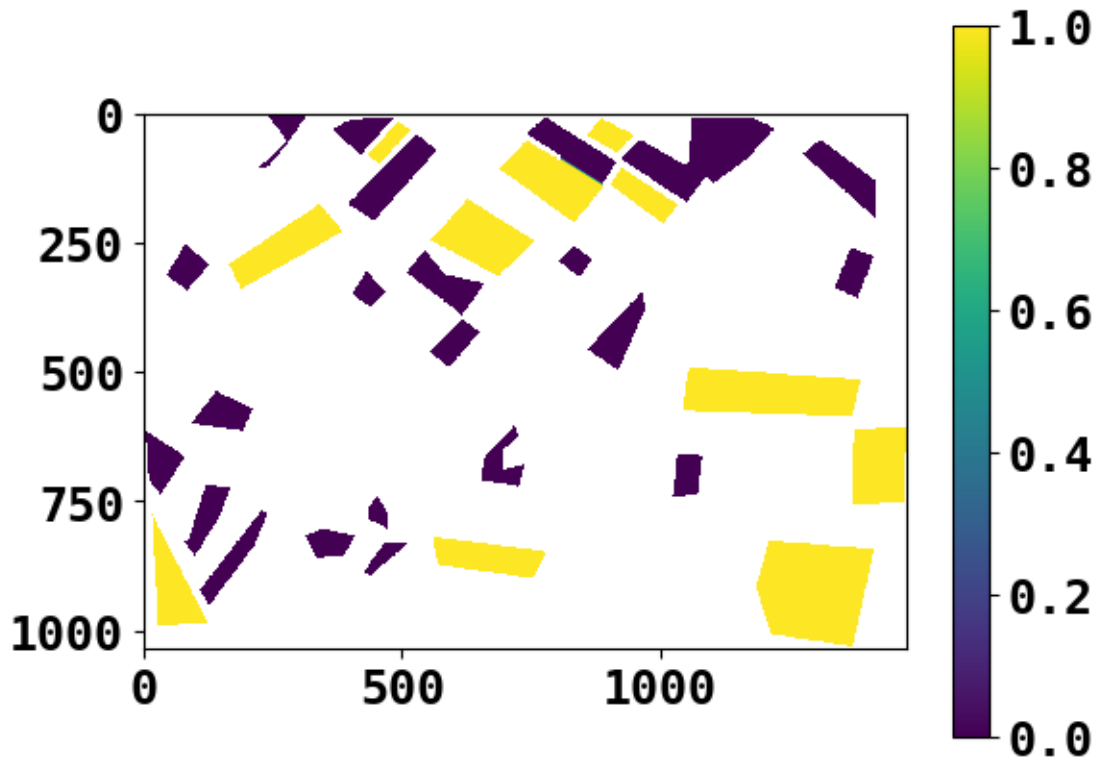


Figure 4.15: Validation Map created using QGIS

4.7 Confusion Matrix

Overall Accuracy:

The frequency with which the classifier properly identifies the data is expressed as the overall accuracy (OA). It is determined by dividing the overall number of samples that were correctly categorised (true positives and true negatives) by the overall number of samples.

$$OA = \frac{TN + TP}{TP + FN + FP + TN} \quad (4.1)$$

User Accuracy:

When a sample belongs to a certain class, the user accuracy (UA) is a measurement of how frequently the classifier correctly recognises that class. It is computed by dividing the total of true positives and false negatives for a given class by the number of true positives for that class.

$$UA_i = \frac{TP_i}{TP_i + FN_i} \quad (4.2)$$

Producer Accuracy:

When the real class is that particular class, the producer accuracy (PA) is a measurement of how frequently the classifier correctly identifies that particular class. It is determined by dividing the total of true positives and false positives for a given class by the number of true positives for that class.

$$PA_i = \frac{TP_i}{TP_i + FP_i} \quad (4.3)$$

Kappa Coefficient:

The degree of agreement that may happen by chance is taken into account when calculating the kappa coefficient, which measures the agreement between the true and projected class labels. It has a range of -1 to 1, with values nearer to 1 denoting greater agreement. It is derived by subtracting the marginal totals (sums of rows and columns) from the observed agreement ($TP + TN$) and comparing it to the predicted agreement (based on chance).

$$\kappa = \frac{N(TN + TP) - (FP + TP)(FP + TN)}{N^2 - (FP + TP)(FP + TN)} \quad (4.4)$$

Chapter 5

Results and Discussion

5.1 Sentinel-1

In this study, we evaluated the accuracy and kappa values of Sentinel-1 SAR data for two individual bands, VH and VV, as well as their combinations. The results are summarized in Table 5.1. Overall, the combination of VH and VV bands yielded the highest accuracy (VH/VV) and kappa values.

Table 5.1: Summary of Accuracy Analysis of Sentinel-1

Sentinel-1	Hansen's GFC Map (Accuracies in %)				QGIS Ground Truth	
Bands	Overall Accuracy(%)	Kappa	User Accuracy (%)	Producer Accuracy (%)	Overall Accuracy(%)	Kappa
VV	73	0.45	69	83	71	0.41
VH	84	0.49	78	86	67	0.33
VH/VV	85	0.69	83	91	74	0.40
$VH/[VV(VH - VV)]$	59	0.18	57	61	--	--
$(VH - VV)/(VH + VV)$	55	0.11	55	60	--	--

However, further in-depth analysis of the individual bands and their combinations is provided below along with the change maps.

5.1.1 VV band - Sentinel - 1

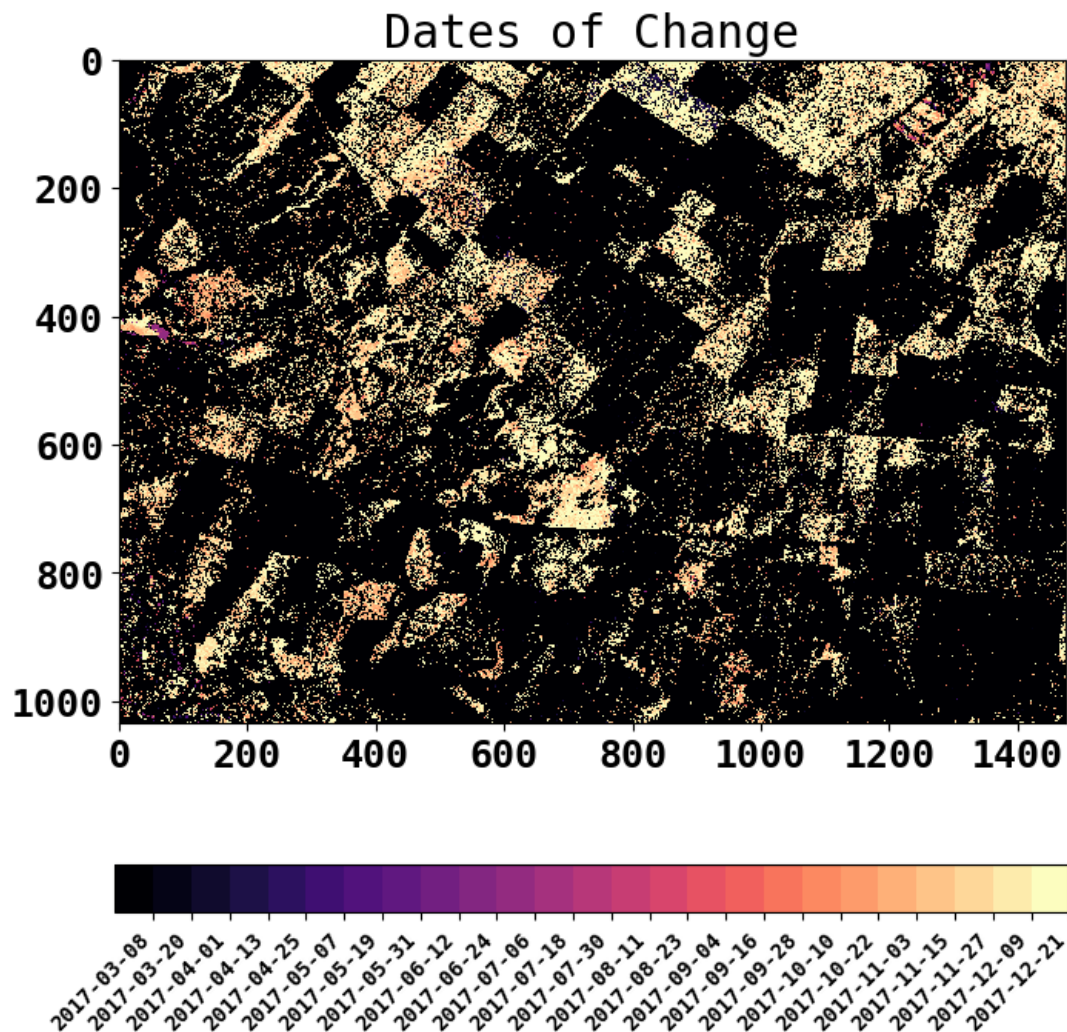


Figure 5.1: Change map obtained from Sentinel - 1 - VV Band

The VV band here is more sensitive to vertical structures compared to the VH band. This is because the VV polarization corresponds to vertical transmit and receive signals. Therefore, the VV band is more sensitive to the changes in trunk and upper branches of vegetation, which tend to have a more vertical orientation. As a result, a change map generated using the VV band can provide a more detailed and accurate representation of changes in vegetation cover, particularly those related to the vertical structures of trees and vegetation.

Normalized confusion matrix:

1.00 0.45

0.20 0.73

Accuracy: 73%

Kappa value: 0.45

User accuracy: 69%

Producer accuracy: 83%

5.1.2 VH band - Sentinel - 1

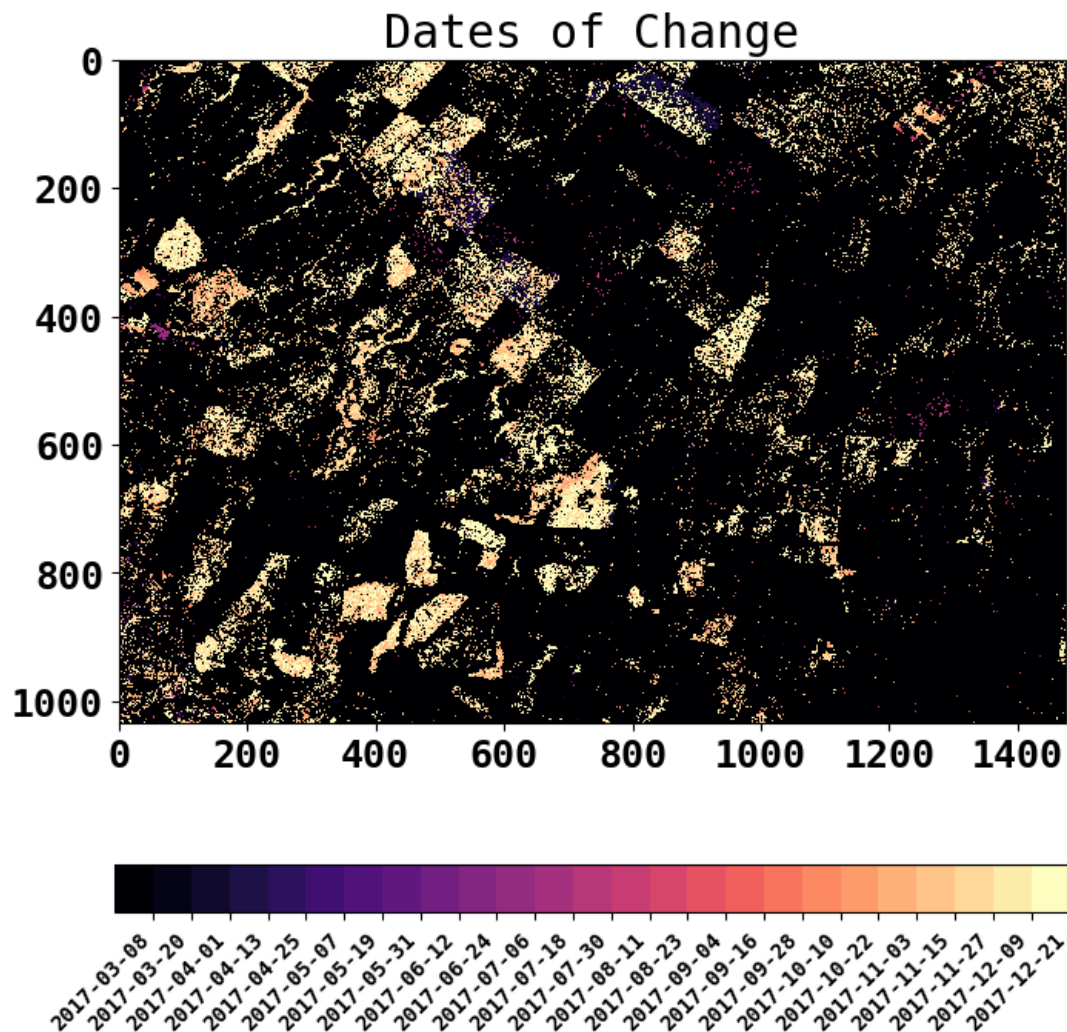


Figure 5.2: Change map obtained from Sentinel - 1 - VH Band

The VH (Vertical and Horizontal) band in SAR imaging is more sensitive to horizontal structures such as the canopy and the horizontal branches of vegetation. This is because the polarization of the signal is transmitted vertically and received horizontally, which makes it more sensitive to changes in the orientation of the canopy and the orientation of the branches relative to the radar beam. As a result, the VH band can be useful in identifying changes in the canopy and the horizontal branches of vegetation, which tend to be more horizontally oriented.

Normalized confusion matrix:

1.00 0.22

0.11 0.89

Accuracy: 85%

Kappa value: 0.49

User accuracy: 78%

Producer accuracy: 86%

5.1.3 VH / VV - Sentinel - 1

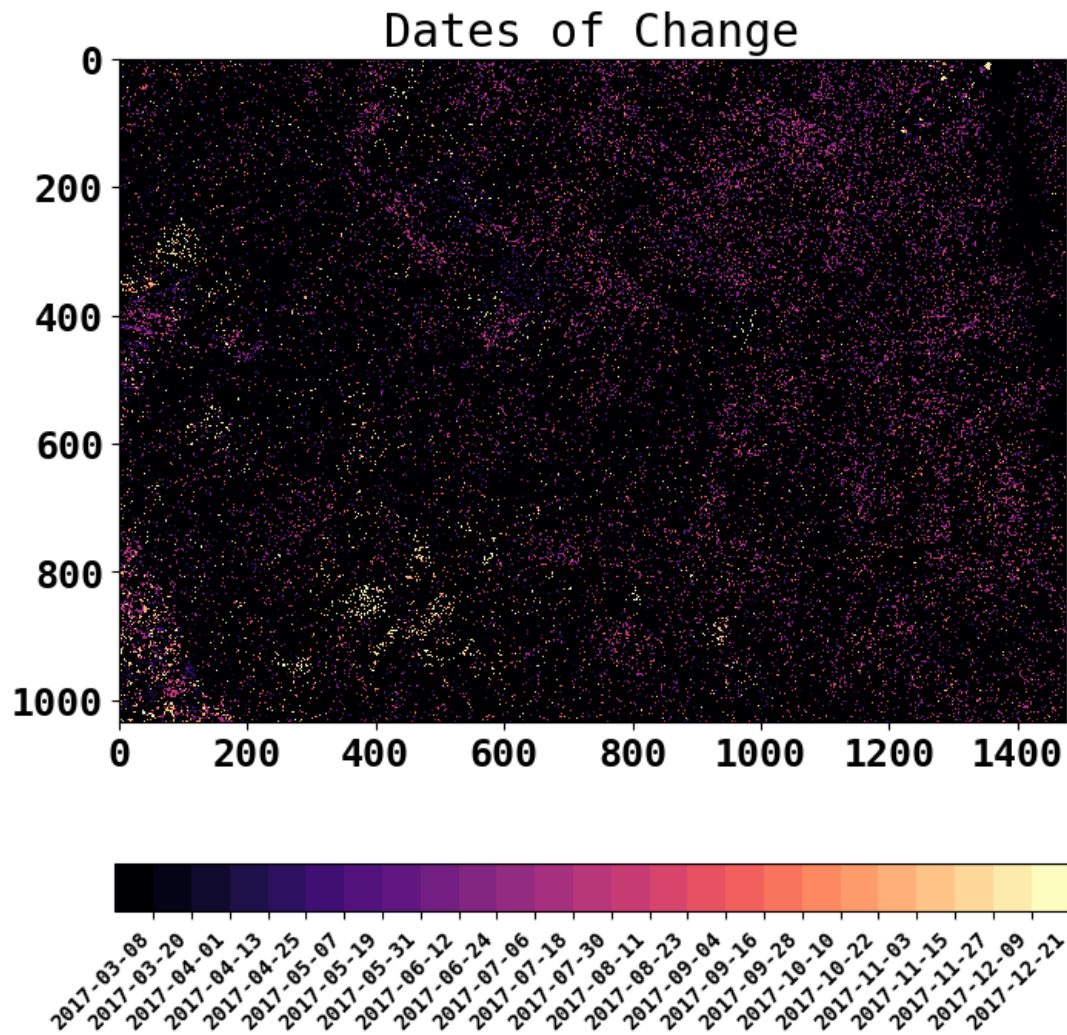


Figure 5.3: Change map obtained from Sentinel - 1 - VH/VV

The VV/VH ratio of Sentinel-1 is particularly significant for forest and vegetation mapping as it provides a measure of the structural complexity and moisture content of vegetation. This ratio is better than individual VV or VH readings as it takes into account the differences in sensitivity of the two polarizations to different types of forest and vegetation structures. In addition, the ratio is less affected by speckle noise, which can be a problem with individual readings, allowing for more accurate mapping of forest cover changes over time.

Normalized confusion matrix:

1.00 0.20

0.10 0.70

Accuracy: 85%

Kappa value: 0.69

User accuracy: 83%

Producer accuracy: 91%

5.1.4 $VH/[VV(VH-VV)]$ and $(VH-VV)/(VH+VV)$ - Sentinel - 1

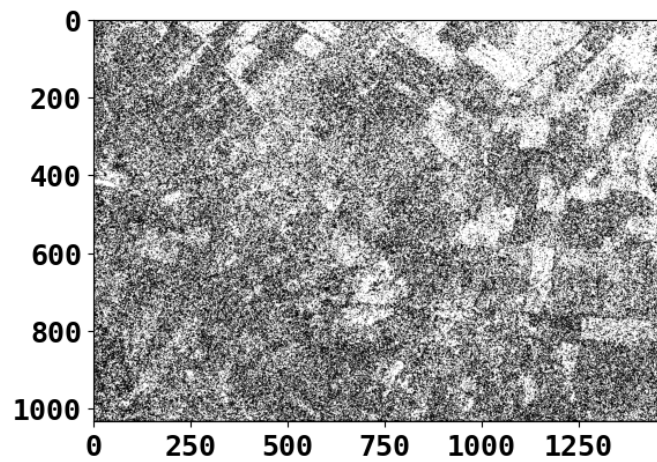


Figure 5.4: Change map for $VH/[VV(VH-VV)]$

Despite varying the threshold, the $VH/[VV(VH-VV)]$ ratio did not yield any significant results in detecting changes in forest cover. The accuracy of the results was low, despite using more manual and statistical methods to vary the thresholds.

Accuracy - 59 %

Kappa Coefficient - 0.18

For $(VH-VV)/(VH+VV)$ -

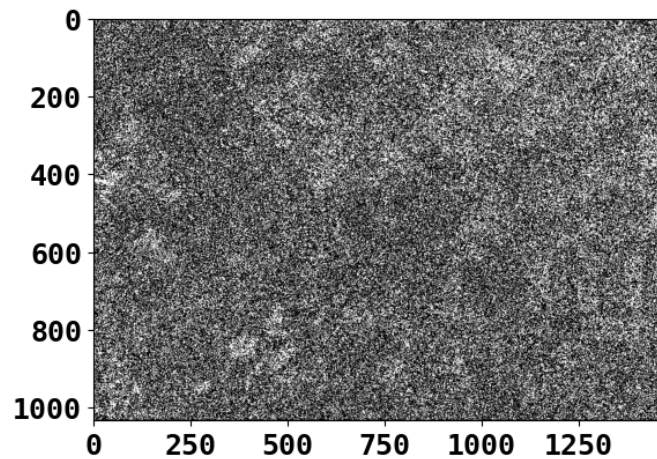


Figure 5.5: Change map for $(VH-VV)/(VH+VV)$

Similar to $(VH-VV)/(VH+VV)$, the accuracy obtained in this case was very low, despite varying the threshold.

Accuracy - 55 %

Kappa Coefficient - 0.11

5.2 Sentinel-2

In this study, we evaluated the accuracy and kappa values of Sentinel-2 data for 4 individual bands, namely Band-4, Band-5, Band-6, Band-8, and NDVI, as shown in Table 5.2 . Overall, Band-6 had the highest accuracy and kappa values, with an accuracy of 75.17 % and kappa of 0.42.

Table 5.2: Summary of Accuracy Analysis of Sentinel-2

Sentinel-2	Hansen's GFC Map (Accuracies in %)				QGIS Ground Truth	
Bands	Overall Accuracy (%)	Kappa	User Accuracy (%)	Producer Accuracy (%)	Overall Accuracy (%)	Kappa
Band 4	62	0.21	69	67	54	0.10
Band 5	62	0.23	59	67	57	0.12
Band 6	73	0.46	70	80	75	0.40
Band 8	71	0.36	76	78	72	0.34
NDVI	64	0.24	69	73	62	0.19

However, further in-depth analysis of the individual bands and their combinations is provided below along with the change maps.

5.2.1 Band 4 - Sentinel - 2

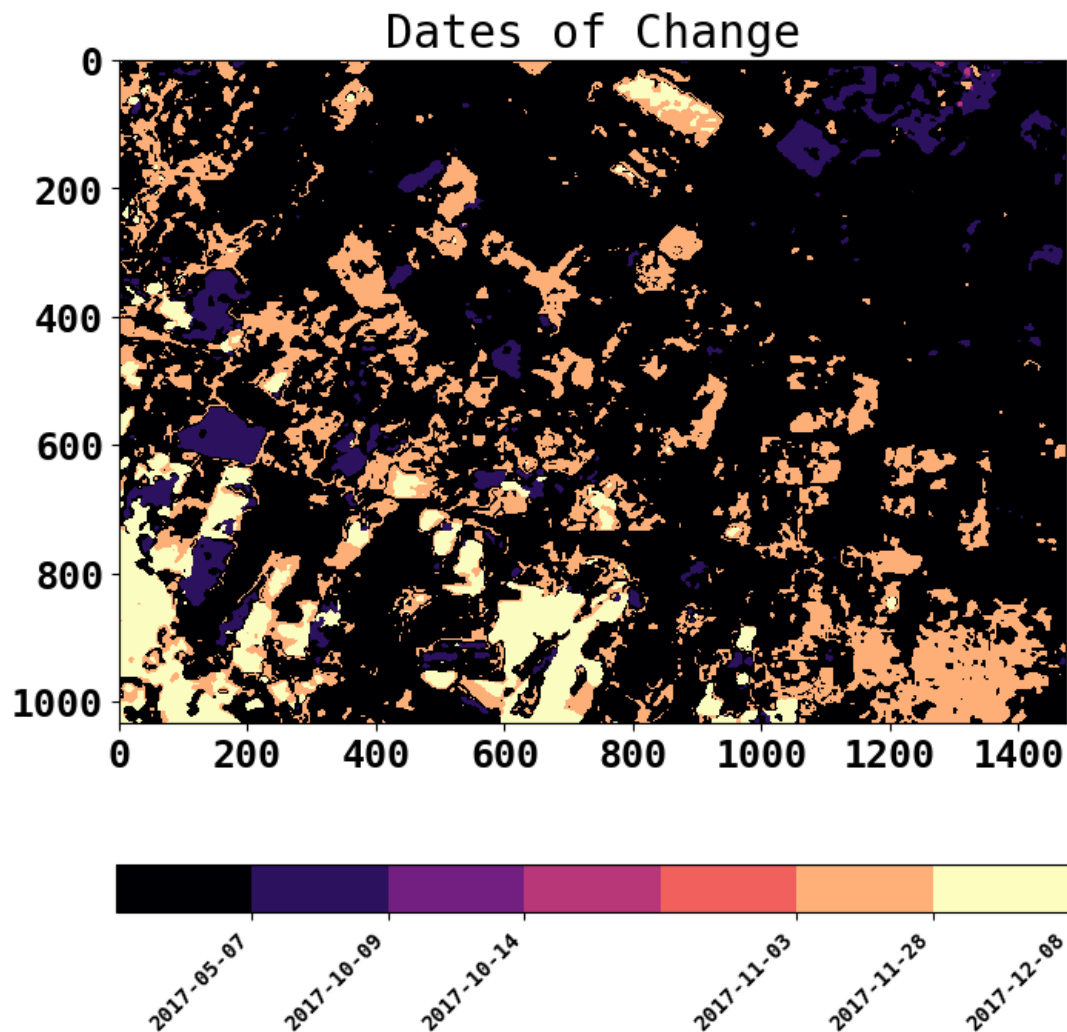


Figure 5.6: Change map obtained from Sentinel-2, Band 4

Sentinel-2's band 4 is sensitive to red-edge radiation, which can be useful for detecting changes in forest cover due to deforestation. As healthy vegetation reflects more red-edge radiation than unhealthy or bare land, changes in the red-edge reflectance can indicate changes in forest cover. By analyzing the change in band 4 reflectance over time, a change map can be generated to identify areas where deforestation has occurred. The interaction of band 4 with the forest is crucial for accurate detection of changes. In a healthy forest, band 4 reflectance will be relatively stable over time, while in deforested areas, there will be a significant decrease in reflectance due to the loss of vegetation cover.

Normalized confusion matrix:

1.00 0.45

0.50 0.53

Accuracy: 62%

Kappa value: 0.21

User accuracy: 69%

Producer accuracy: 67%

5.2.2 Band 5 - Sentinel - 2

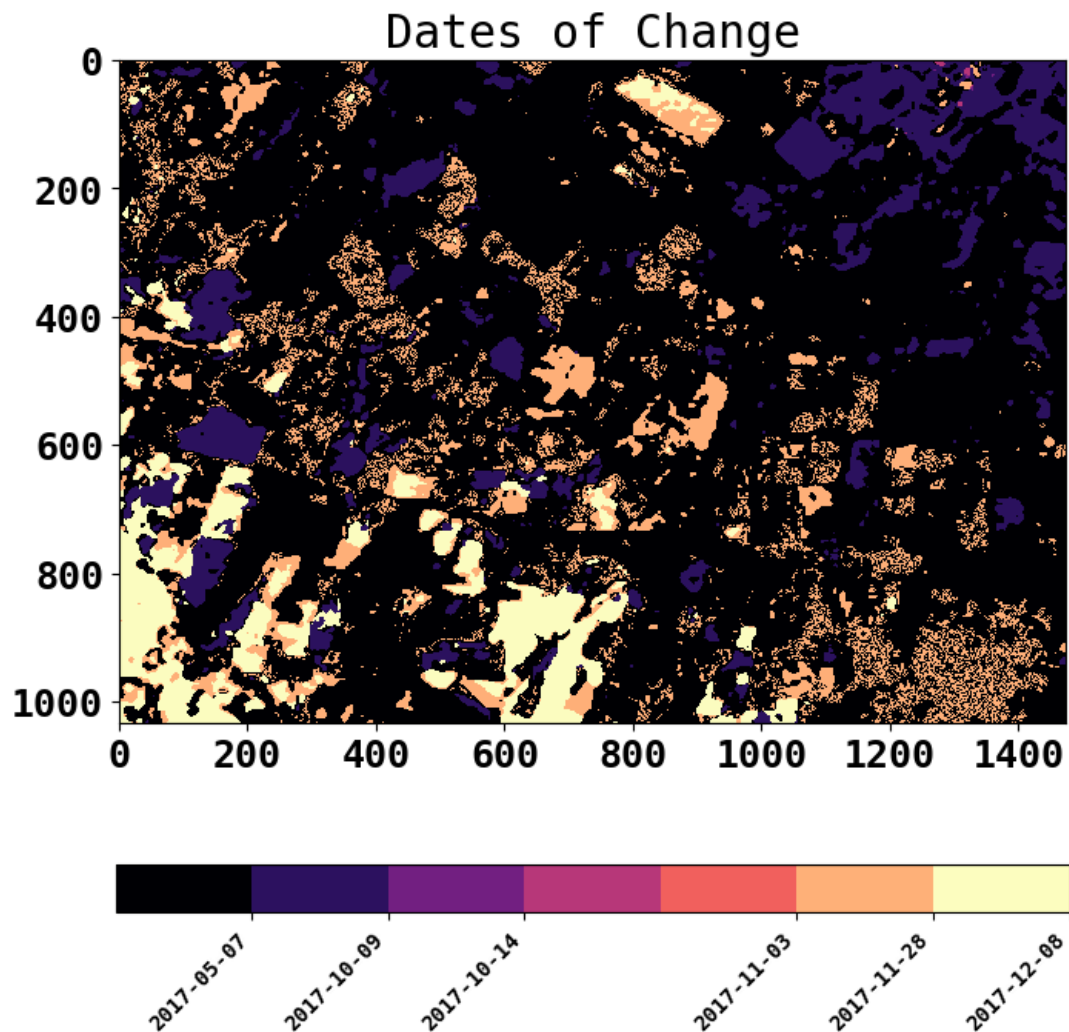


Figure 5.7: Change map obtained from Sentinel - 2, Band 5

Band 5 is sensitive to shortwave infrared radiation and is mainly used for detecting moisture content. While changes in vegetation water stress can indicate changes in forest health, it may not be as reliable for detecting deforestation as band 4. The interaction of band 5 with the forest can provide information on vegetation water content and health, which can be useful for monitoring forest health and identifying areas where deforestation may be occurring.

Normalized confusion matrix:

1.00 0.70

0.50 0.92

Accuracy: 62%

Kappa value: 0.23

User accuracy: 59%

Producer accuracy: 67%

5.2.3 Band 6 - Sentinel - 2

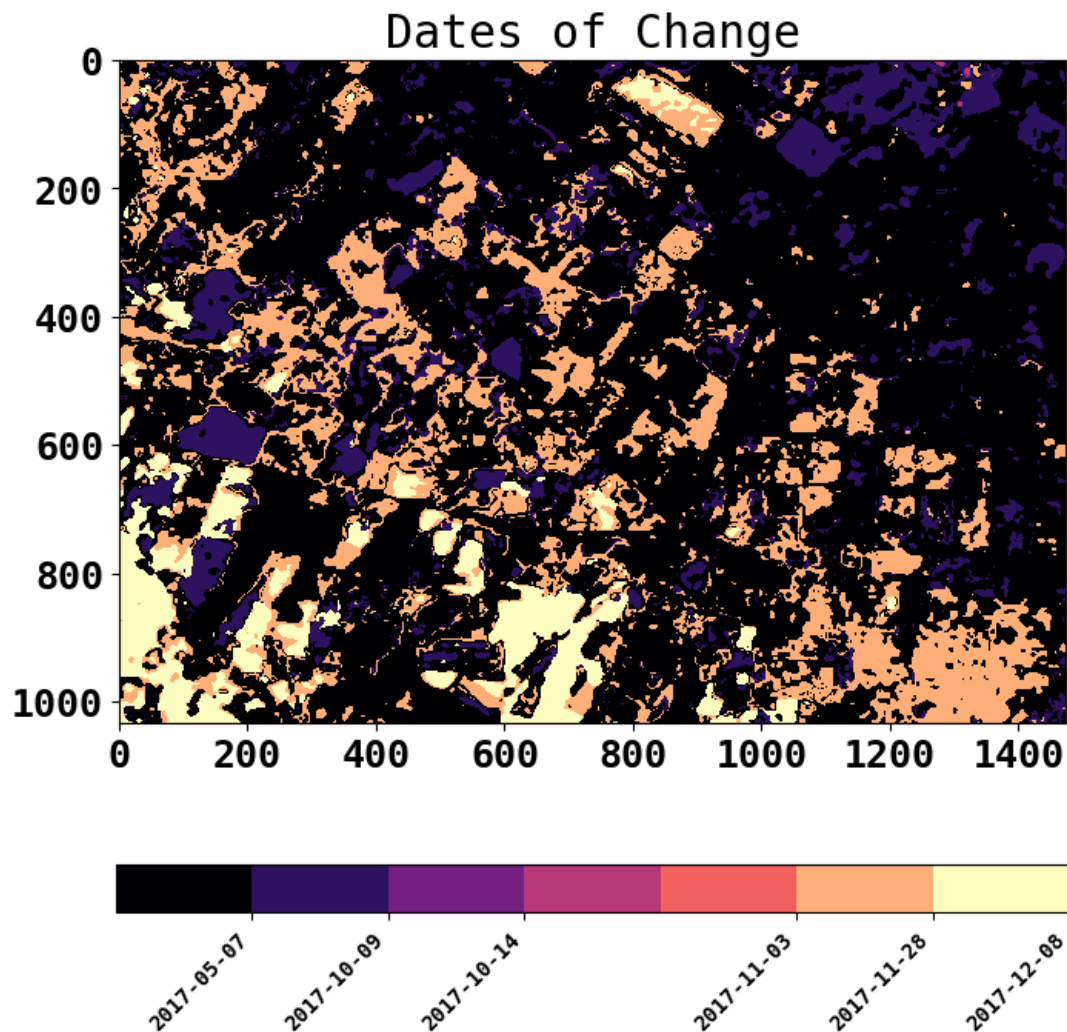


Figure 5.8: Change map obtained from Sentinel - 2 - Band 6

The interaction of band 6 with the forest can provide information on the amount of water stored in the leaves and stems of the vegetation, which can indicate the health and vigor of the forest. Healthy vegetation typically has high moisture content, while dry vegetation can indicate stress or damage. In forests, the moisture content of the vegetation can vary depending on factors such as seasonality, vegetation type, and canopy structure. By analyzing changes in the moisture content of the vegetation over time, it is possible to detect changes in forest health and identify areas where deforestation or other disturbances may be occurring.

Normalized confusion matrix:
1.00 0.42
0.25 0.82
Accuracy: 73%
Kappa value: 0.46
User accuracy: 70%
Producer accuracy: 80%

5.2.4 Band 8 - Sentinel - 2

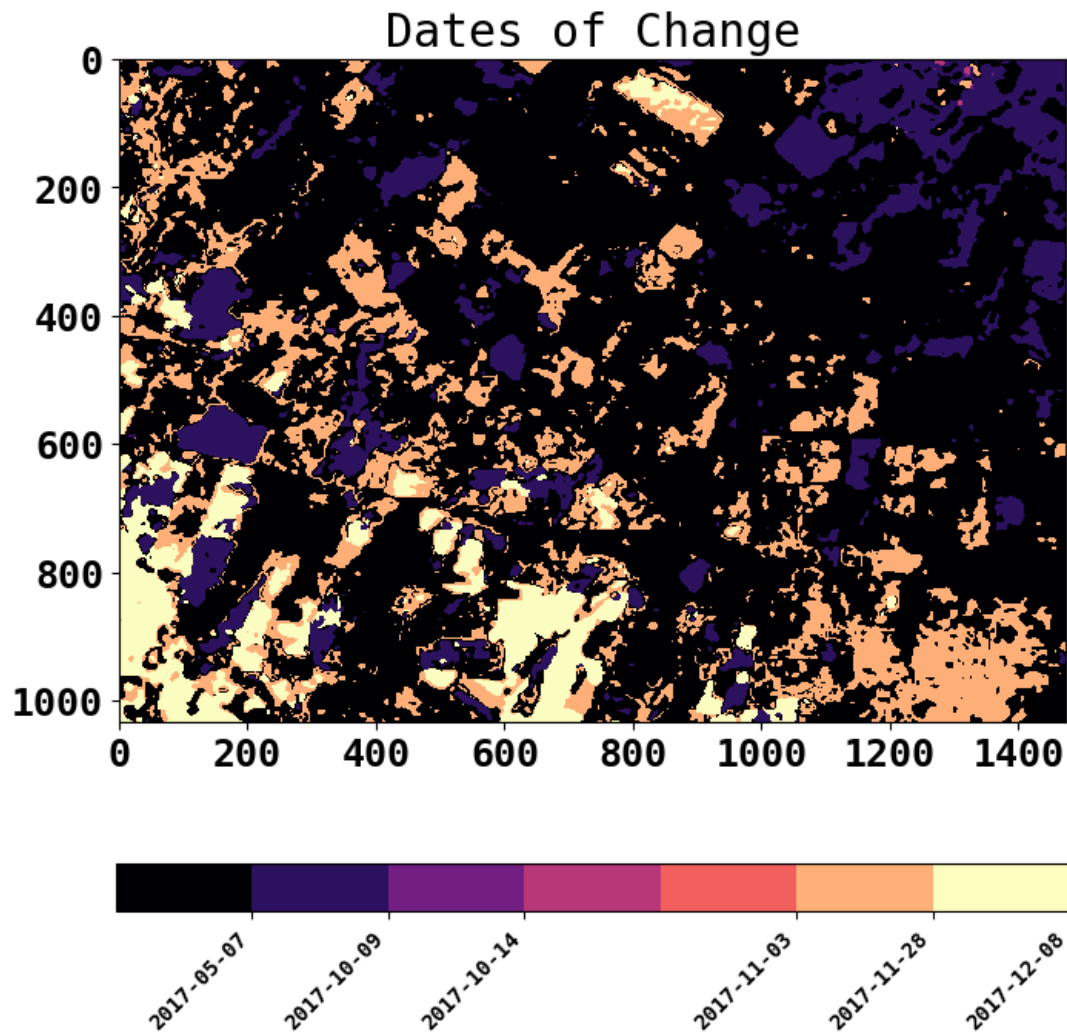


Figure 5.9: Change map obtained from Sentinel - 2 - Band 8

Sentinel-2's band 8 is sensitive to the near-infrared radiation and is widely used in remote sensing applications for monitoring land use and land cover changes. In particular, band 8 can be used for detecting changes in vegetation cover due to deforestation. The interaction of band 8 with the forest can provide information on the density and health of the vegetation, which can be used to detect changes in forest cover over time. In healthy vegetation, band 8 reflectance is relatively high due to the high density of leaves and the chlorophyll content in the plant cells. However, in areas where deforestation has occurred, there will be a significant decrease in band 8 reflectance due to the loss of vegetation cover.

Normalized confusion matrix:

1.00 0.32

0.28 0.44

Accuracy: 71%

Kappa value: 0.36

User accuracy: 76%

Producer accuracy: 78%

5.2.5 NDVI (Band 8 - Band 4 / Band 8 + Band 4) - Sentinel - 2

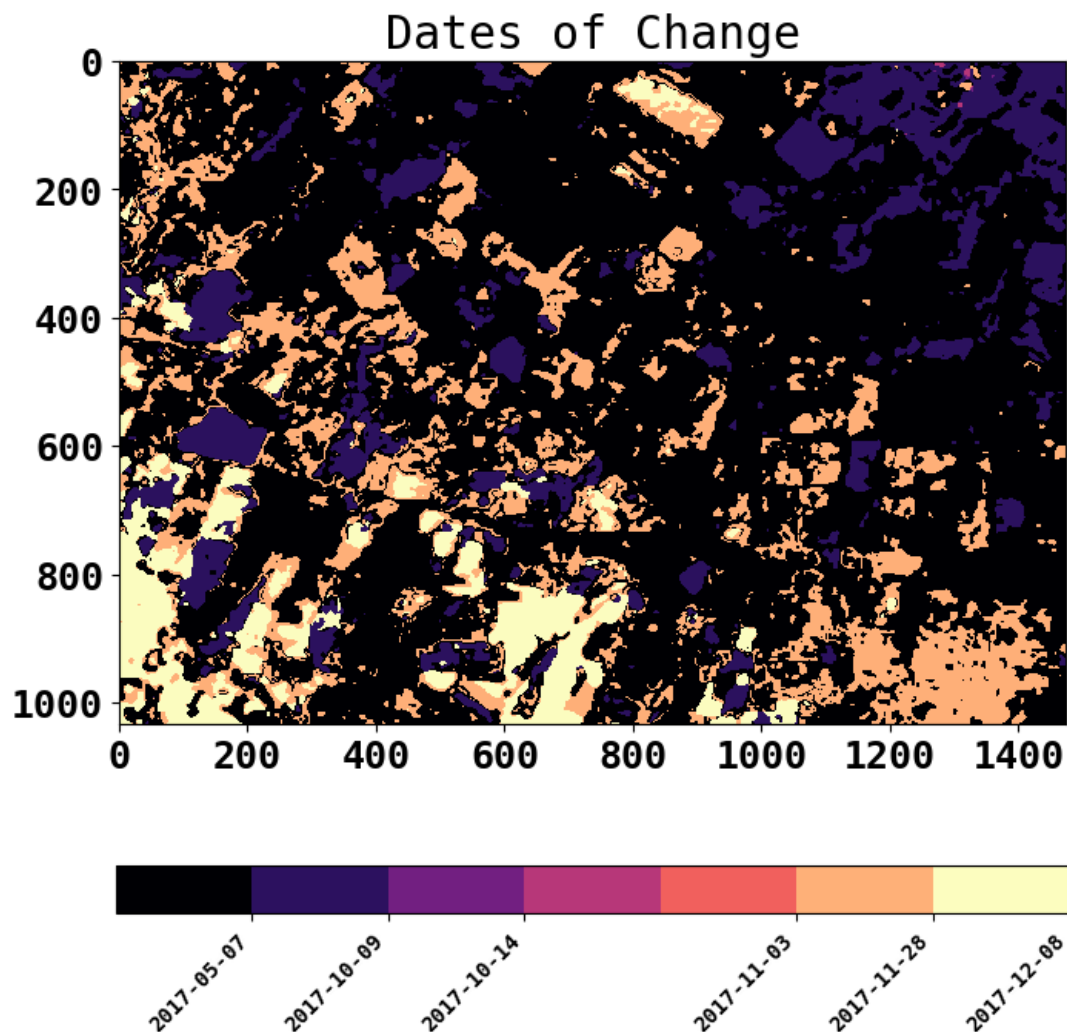


Figure 5.10: Change map obtained from Sentinel - 2 - NDVI

NDVI is calculated by taking the difference between the near-infrared (band 8) and red (band 4) reflectance and dividing it by their sum. The use of NDVI for generating change maps for deforestation can be an effective approach, as changes in vegetation cover due to deforestation will result in a significant decrease in NDVI values over time. The NDVI change map can be used to identify areas where deforestation has occurred, allowing for effective management and conservation of forest resources.

Normalized confusion matrix:

1.00 0.45

0.36 0.45

Accuracy: 64%

Kappa value: 0.24

User accuracy: 69%

Producer accuracy: 73%

5.3 Accuracy Analysis Based on Type of Forest

Following an analysis of change detection accuracy across different bands of Sentinel-1 and Sentinel-2, the accuracy of identifying Forest Type and Forest Species was determined. A forest type refers to a specific classification of forest based on its ecological and biological characteristics, such as the dominant tree species, forest structure, and climate conditions. For instance, Dry Shivalik Sal and Moist Tarai Sal are examples of forest types found in India, where the dominant tree species in each type is Sal (*Shorea robusta*), but the former is characterized by dry and hilly terrain, while the latter is found in lowland areas with a high level of moisture. Forest types are useful in understanding the different ecosystems, their biodiversity, and the services they provide, and can aid in the development of sustainable forest management practices. Three distinct forest types were selected from the study area, and the behavior of multiple bands of Sentinel-1 and Sentinel-2 was analyzed, along with accuracy assessments for each of these forest types.

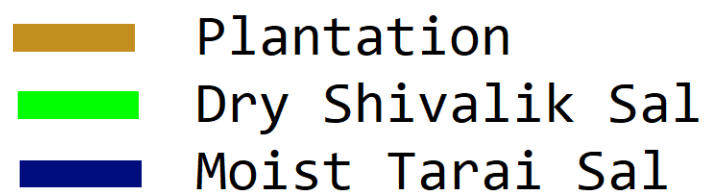
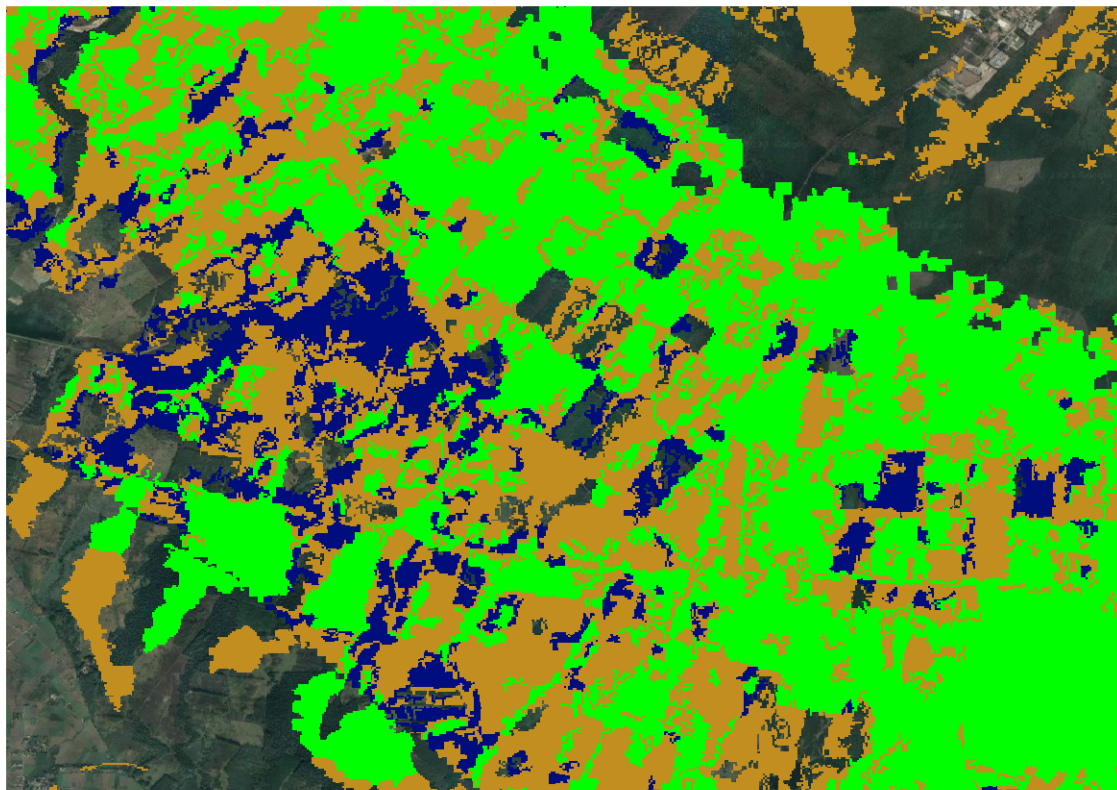


Figure 5.11: Types of forests in the Area of Interest

5.3.1 Plantation

Table 5.3: Accuracy Analysis of Plantation type of trees in the forest - Accuracy in %

Sentinel 1 - Plantation		
Band	Accuracy (%)	Kappa
VV	87	0.44
VH	88	0.77
VH/VV	81	0.42
VH/[VV(VH-VV)]	72	0.38
(VH-VV)/(VH+VV)	84	0.40

Normalized confusion matrix:
 1.00 0.06
 0.20 0.94
 Accuracy: 0.88
 Kappa value: 0.77
 User accuracy: 0.95
 Producer accuracy: 0.83

Sentinel 2 - Plantation		
Band	Accuracy (%)	Kappa
Band 4	76	0.45
Band 5	74	0.45
Band 6	83	0.65
Band 8	78	0.32
NDVI	70	0.29

Normalized confusion matrix:
 1.00 0.16
 0.18 0.69
 Accuracy: 0.83
 Kappa value: 0.65
 User accuracy: 0.86
 Producer accuracy: 0.84

Based on our analysis, the forest type under consideration demonstrated the highest accuracy and kappa values when using the VH band of Sentinel-1 and Band 6 of Sentinel-2. Specifically, the VH band of Sentinel-1 yielded the highest accuracy and kappa values.

5.3.2 Dry Shivalik Sal

Table 5.4: Accuracy Analysis of Dry Shivalik Sal type of trees in the forest

Sentinel 1 - Dry Shivalik Sal		
Band	Accuracy (%)	Kappa
VV	67	0.32
VH	76	0.41
VH/VV	77	0.44
VH/[VV(VH-VV)]	63	0.27
(VH-VV)/(VH+VV)	80	0.59

Normalized confusion matrix:
 1.00 0.23
 0.21 0.75
 Accuracy: 0.80
 Kappa value: 0.59
 User accuracy: 0.81
 Producer accuracy: 0.83

Sentinel 2 - Dry Shivalik Sal		
Band	Accuracy (%)	Kappa
Band 4	71	0.39
Band 5	75	0.50
Band 6	72	0.40
Band 8	68	0.38
NDVI	62	0.22

Normalized confusion matrix:
 1.00 0.37
 0.22 0.76
 Accuracy: 0.75
 Kappa value: 0.50
 User accuracy: 0.73
 Producer accuracy: 0.82

Based on our analysis, the forest type under consideration demonstrated the highest accuracy and kappa values when using the VH/VV of Sentinel-1 and Band 5 of Sentinel-2. Both of these bands provide almost equally good accuracy.

5.3.3 Moist Tarai Sal

Table 5.5: Accuracy Analysis of Moist Tarai Sal type of trees in the forest

Sentinel 1 - Moist Tarai Sal		
Band	Accuracy (%)	Kappa
VV	68	0.29
VH	7	0.39
VH/VV	78	0.56
VH/[VV(VH-VV)]	46	0.22
(VH-VV)/(VH+VV)	34	0.01

Normalized confusion matrix:
 1.00 0.27
 0.20 0.73
 Accuracy: 0.78
 Kappa value: 0.56
 User accuracy: 0.79
 Producer accuracy: 0.83

Sentinel 2 - Moist Tarai Sal		
Band	Accuracy (%)	Kappa
Band 4	75	0.42
Band 5	73	0.40
Band 6	84	0.68
Band 8	39	0.12
NDVI	44	0.17

Normalized confusion matrix:
 0.83 0.15
 0.20 1.00
 Accuracy: 0.84
 Kappa value: 0.68
 User accuracy: 0.84
 Producer accuracy: 0.81

Based on our analysis, the forest type under consideration demonstrated the highest accuracy and kappa values when using the VH/VV of Sentinel-1 and Band 6 of Sentinel-2. Specifically, the Band-6 of Sentinel-2 yielded the highest accuracy and kappa values.

5.4 Accuracy Analysis Based on the Species

In order to gain a more comprehensive understanding of the forested region under study, we conducted a species-level analysis on the three most abundant tree species: Teak, Cottonwood / Poplar, and Mixed Plantation. These species were selected for analysis due to their prevalence in the area and their ecological significance. The forested region is composed of numerous compartments, each with multiple species present. Our analysis focused on the compartments where these three species were found in abundance. By analyzing the accuracy of detection of these species within each compartment, we were able to gain insights into the performance of different bands of Sentinel - 1 and Sentinel - 2 for detecting each species. This analysis helps us to better understand the distribution and abundance of each species within the region.

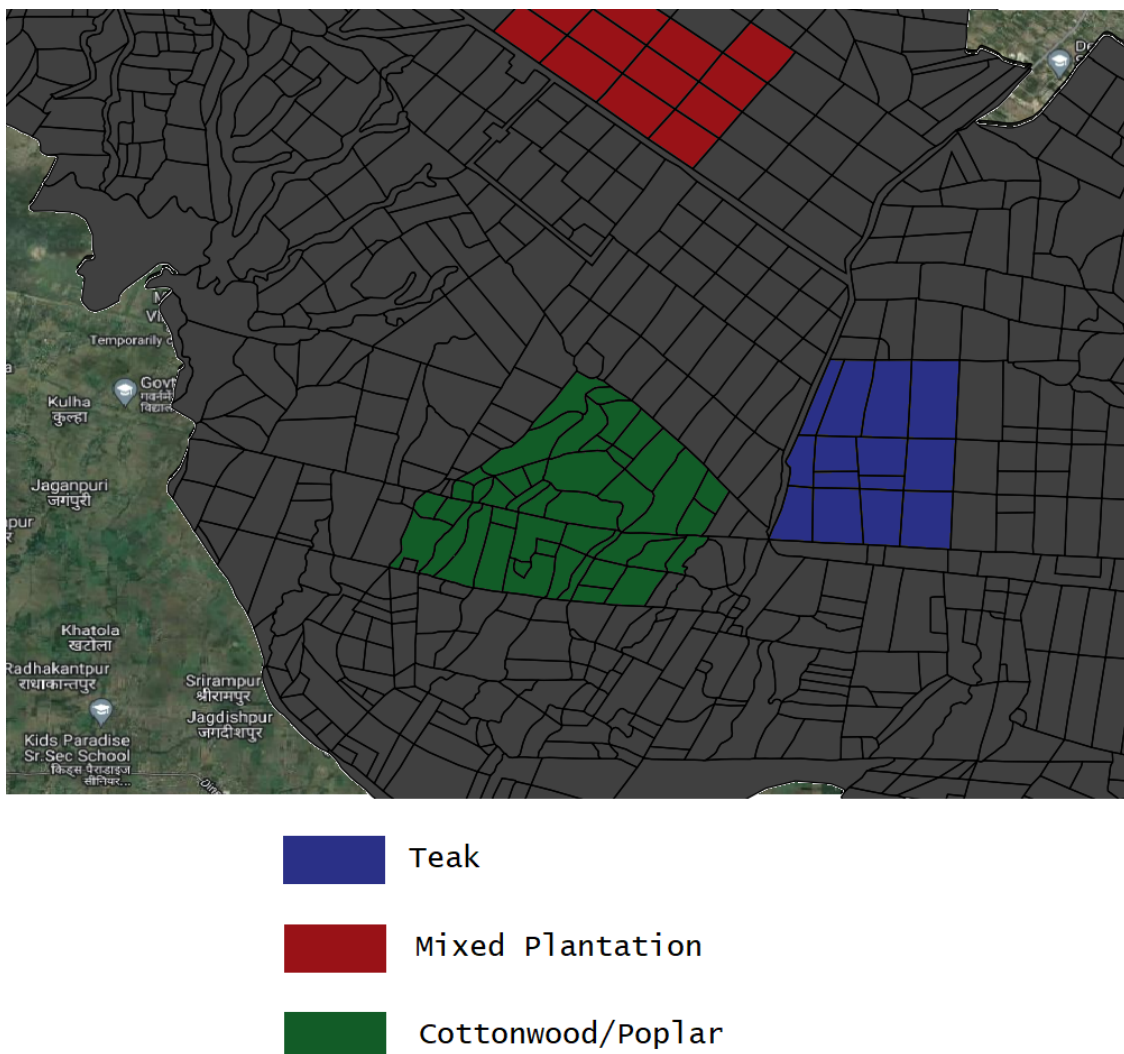


Figure 5.12: Distribution of various species in the forest, the lines depict the separation between 2 compartments

5.4.1 Teak

Table 5.6: Accuracy Analysis of Teak trees in the forest

Sentinel 1 - Teak		
Band	Accuracy (%)	Kappa
VV	77	0.40
VH	82	0.64
VH/VV	73	0.37
VH/[VV(VH-VV)]	60	0.32
(VH-VV)/(VH+VV)	63	0.38

Normalized confusion matrix:
 0.82 0.18
 0.22 1.00
 Accuracy: 0.82
 Kappa value: 0.64
 User accuracy: 0.82
 Producer accuracy: 0.79

Sentinel 2 - Teak		
Band	Accuracy (%)	Kappa
Band 4	71	0.37
Band 5	76	0.52
Band 6	74	0.41
Band 8	68	0.22
NDVI	60	0.17

Normalized confusion matrix:
 1.00 0.35
 0.15 0.62
 Accuracy: 0.76
 Kappa value: 0.52
 User accuracy: 0.74
 Producer accuracy: 0.87

Based on our analysis, the forest species under consideration demonstrated the highest accuracy and kappa values when using the VH of Sentinel-1 and Band 5 of Sentinel-2. Specifically, the VH of Sentinel-1 yielded the highest accuracy and kappa values.

5.4.2 Cottonwood / Poplar

Table 5.7: Accuracy Analysis of Cottonwood / Poplar trees in the forest,

Sentinel 1 - Cottonwood / Poplar		
Band	Accuracy	Kappa
VV	85	0.69
VH	82	0.47
VH/VV	83	0.44
VH/[VV(VH-VV)]	70	0.30
(VH-VV)/(VH+VV)	79	0.38

Normalized confusion matrix:
 1.00 0.20
 0.07 0.53
 Accuracy: 0.85
 Kappa value: 0.69
 User accuracy: 0.84
 Producer accuracy: 0.94

Sentinel 2 - Cottonwood / Poplar		
Band	Accuracy (%)	Kappa
Band 4	65	0.36
Band 5	63	0.35
Band 6	68	0.34
Band 8	66	0.34
NDVI	66	0.34

Normalized confusion matrix:
 1.00 0.42
 0.29 0.54
 Accuracy: 0.68
 Kappa value: 0.34
 User accuracy: 0.70
 Producer accuracy: 0.78

Based on our analysis, the forest type under consideration demonstrated the highest accuracy and kappa values when using the VV of Sentinel-1 and Band 6 of Sentinel-2. Specifically, the VV Band of Sentinel-1 yielded the highest accuracy and kappa values.

5.4.3 Mixed-Plantation

Table 5.8: Accuracy Analysis of mixed plantation type of trees in the forest, accuracy in %

Sentinel 1 - Mixed Plantation		
Band	Accuracy	Kappa
VV	78	0.37
VH	82	0.63
VH/VV	73	0.37
VH/[VV(VH-VV)]	61	0.27
(VH-VV)/(VH+VV)	57	0.19

Normalized confusion matrix:
 1.00 0.18
 0.22 0.80
 Accuracy: 0.82
 Kappa value: 0.63
 User accuracy: 0.85
 Producer accuracy: 0.82

Sentinel 2 - Mixed Plantation		
Band	Accuracy	Kappa
Band 4	81	0.61
Band 5	81	0.56
Band 6	84	0.68
Band 8	81	0.59
NDVI	82	0.61

Normalized confusion matrix:
 1.00 0.16
 0.18 0.80
 Accuracy: 0.84
 Kappa value: 0.68
 User accuracy: 0.86
 Producer accuracy: 0.85

Based on our analysis, the forest type under consideration demonstrated the highest accuracy and kappa values when using the VH of Sentinel-1 and Band 6 of Sentinel-2. Specifically, the VH of Sentinel-1 yielded the highest accuracy and kappa values.

Chapter 6

Summary & Conclusion

In conclusion, the results of this study demonstrate the potential of Sentinel - 1 and Sentinel - 2 data for high-resolution monitoring and detection of forest logging and deforestation. The use of both Sentinel - 1 and Sentinel - 2 data provides complementary information, allowing for more comprehensive and accurate detection of forest changes. Our analysis revealed that certain bands and combinations of bands provided higher accuracy of change detection, highlighting the importance of careful selection of data for monitoring purposes. The results of this study provide insights into the distribution and abundance of different forest types and tree species, which can inform effective forest management and conservation strategies. Overall, the use of Sentinel - 1 and Sentinel - 2 data for forest monitoring has significant implications for sustainable management of natural resources and conservation efforts.

Summary of Accuracy obtained for Forest-Types and Species - Higher ones are highlighted:

Table 6.1: Summary of Type and Species-wise accuracy

Highest Accuracies Obtained (%)		Sentinel 1	Sentinel 2
Forest Type	Plantation / TOF	89.32	82.78
	Dry Shivalik Sal	79.64	77.86
	Moist Tarai Sal	79.29	83.56
Species	Teak	84.37	83.95
	Cottonwood	84.20	68.64
	Mixed-Plantation	86.66	83.95

The analysis of forest types and species using Sentinel - 1 and Sentinel - 2 data revealed interesting insights into the performance of different bands for detecting changes in forest cover. For forest types, Sentinel - 1 showed superior performance for Mixed Plantation/TOF and Dry Shivalik, while certain bands of Sentinel - 2 provided better outputs for Mixed Tarai. However, overall Sentinel - 1 tended to provide better accuracy than Sentinel - 2 for most of the bands. On the other hand, for forest species, Sentinel - 1 provided better accuracy by a significant margin for Teak and Cottonwood / Poplar, while Sentinel - 2 tended to perform better for Mixed Plantation.

Sentinel-1 through clouds, rain, and fog, allowing for all-weather and day-night monitoring. This capability is especially important for forest and vegetation mapping, as clouds and precipitation frequently cover forested areas, hindering optical satellite data

acquisition. Sentinel-1 SAR data can detect the structure of vegetation and provide information on the density, height, and biomass of forests, even in areas with dense canopies or tropical forests with limited access due to heavy cloud cover.

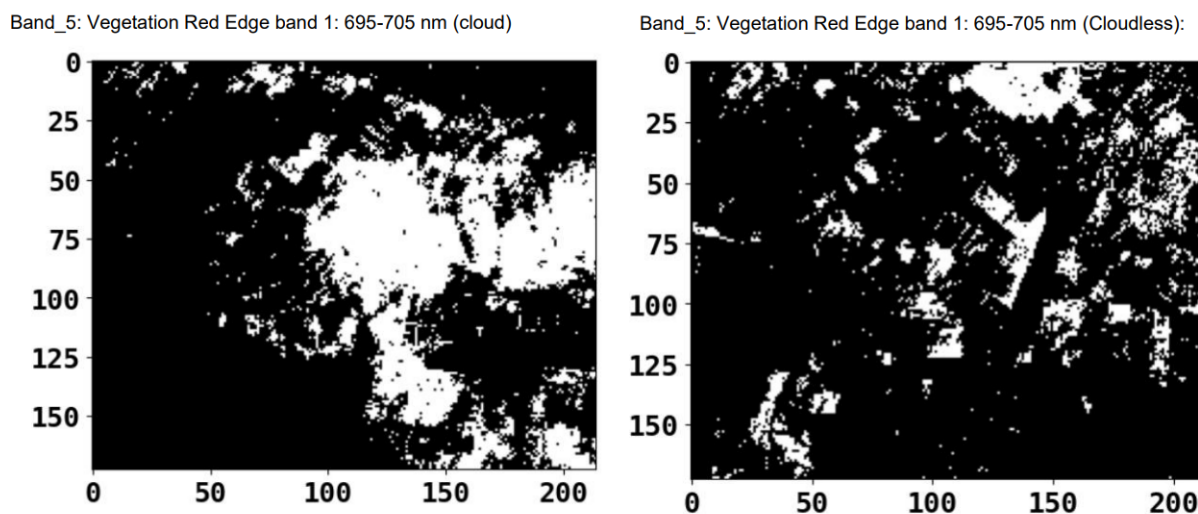


Figure 6.1: Change map obtained from Sentinel - 2 - Band 8 - in presence and absence of cloud cover

On the other hand, Sentinel-2 uses multispectral imaging with 13 spectral bands that cover the visible and near-infrared range, providing high-resolution images of the Earth's surface. However, its readings are affected by cloud cover, causing them to be less reliable than Sentinel-1. Clouds can obscure the surface and lead to errors in the classification of land cover and changes in vegetation over time, making it difficult to monitor deforestation. Moreover, Sentinel-2's data acquisition is limited to daytime operations, which further reduces its effectiveness in monitoring forest and vegetation changes.

Creating a change map for deforestation using Sentinel-2 data requires removing the layers of cloud from the Virtual Raster Tile (VRT) file. This process involves using cloud masks to remove areas that are affected by clouds or shadows, so that only cloud-free pixels are used in the analysis. This can be a challenging and time-consuming task, especially in areas with persistent cloud cover or frequent changes in weather patterns.

In summary, while both Sentinel-1 and Sentinel-2 can be used for forest and vegetation mapping, Sentinel-1's SAR technology allows for all-weather and day-night monitoring, making it more reliable for detecting changes in forest cover and deforestation. Sentinel-2's readings are less accurate and are affected by cloud cover, making it less reliable for monitoring forest and vegetation changes, especially in regions with persistent cloud cover.

References

- [1] M. Marcuccio S.; Votto C.; Ullo S.L. Addabbo, P.; Focareta. Contribution of sentinel-2 data for applications in vegetation monitoring.
- [2] Butchart S. H. Dutson G. Pilgrim J. D. Steininger M. K. Bishop K. D. Mayaux P. Buchanan, G. M. Using remote sensing to inform conservation status assessment: estimates of recent deforestation rates on new britain and the impacts upon endemic birds. biological conservation.
- [3] al. Chiara Aquino, et. Reliably mapping the location, time and magnitude of low-intensity forest disturbance using a simple satellite radar method.
- [4] F.N.; Salvatore M.; Jacobs H.; Schmidhuber J. Federici, S.; Tubiello. New estimates of co2 forest emissions and removals: 1990–2015.
- [5] Anthony J. Lewis Floyd M. Henderson. Principles and applications of imaging radar, manual of remote sensing.
- [6] <https://www.geospatialworld.net/article/change-detection-ofvegetation-cover-using-multi-temporal-remote-sensing-data-and-gis-techniques>. Change detection of vegetation cover, using multi-temporal remote sensing data and gis techniques.
- [7] Carl P Boardman Javier Ruiz-Ramos, Armando Marino. Using sentinel 1-sar for monitoring long term variation in burnt forest areas.
- [8] E.T.; Woo N.; Torres J.; Moll-Rocek-J.; Ehammer-A.; Collins M.; Jepsen M.R.; Fensholt R. Joshi, N.; Mitchard. Mapping dynamics of deforestation and forest degradation in tropical forests using radar satellite data.
- [9] J. Kellndorfer. Using sar data for mapping deforestation and forest degradation.
- [10] Drenou C. Denux J. P. Balent G.- Cheret V. Lambert, J. Monitoring forest decline through remote sensing time series analysis.
- [11] D Manogaran, G.; Lopez. Spatial cumulative sum algorithm with big data analytics for climate change detection.
- [12] G. Manogaran and D. Lopez. The sar handbook comprehensive methodologies for forest monitoring and biomass estimation.
- [13] Hay G. J. Marceau, D. J. Remote sensing contributions to the scale issue. canadian journal of remote sensing.
- [14] J. F. Mas. Monitoring land-cover changes: a comparison of change detection techniques.

- [15] Johnny A. Johannessen Pieter Nel F. Levelt Ramon F. Hanssen Reid et al. Michael Berger, Jose Moreno. Esa's sentinel missions in support of earth system science.
- [16] E.; Williams M. Milodowski, D.; Mitchard. Forest loss maps from regional satellite monitoring systematically underestimate deforestation in two rapidly changing parts of the amazon.
- [17] E. Mitchard. A review of earth observation methods for detecting and measuring forest change in the tropics.
- [18] C.L.; Kulahci M. Montgomery, D.C.; Jennings. Introduction to time series analysis and forecasting.
- [19] Ribeiro Nunes; Meireles Gomes. Forest contribution to climate change mitigation: Management oriented to carbon capture and storage.
- [20] Klaudia Weronika Pała's and Jarosław Zawadzki. Sentinel-2 imagery processing for tree logging observations on the białowie 'za forest world heritage site.
- [21] M.H. Cosh N. Torbick X. Huang S. Kraatz, S. Rose and P. Siqueira. Performance evaluation of uavsar and simulated nisar data for crop/noncrop classification over stoneville, ms.
- [22] Josef Kellndorfer Michael H. Cosh Nathan Torbick Xiaodong Huang Paul Siqueira Shannon Rose, Simon Kraatz. Evaluating nisar's cropland mapping algorithm over the conterminous united states using sentinel-1 data.
- [23] Ramon Torres. The sentinel-1 mission and its application capabilities.
- [24] Iain H. Woodhouse. Introduction to microwave remote sensing.
- [25] Wigneron Moisy Catry Baup Hamunyela Riazanoff Ygorra B., Frappart F. Deforestation monitoring using sentinel-1 sar images in humid tropical areas.
- [26] Josef Cihlar Michael E. Schaepman Glenda García-Santos Richard Fernandes Michael Berger. Zbyněk Malenovský, Helmut Rott. Sentinels for science: Potential of sentinel-1, -2, and -3 missions for scientific observations of ocean, cryosphere, and land.